On the anti-diagonal filtration for the Heegaard Floer chain complex of a branched double-cover

Eamonn Tweedy

September 16, 2011

Abstract

Seidel and Smith introduced the graded fixed-point symplectic Khovanov cohomology group $Kh_{symp,inv}(K)$ for a knot $K \subset S^3$, as well as a spectral sequence converging to the Heegaard Floer homology group $\widehat{HF}(\Sigma(K)\#(S^2 \times S^1))$ with E_1-page isomorphic to a factor of $Kh_{symp,inv}(K)$ [18]. There the authors proved that $Kh_{symp,inv}$ is a knot invariant. We show here that the higher pages of their spectral sequence are knot invariants also.

1 Introduction

Heegaard Floer homology was introduced by Ozsváth and Szabó in [10], and has proven to be a very useful tool in studying manifolds of dimensions three and four. We'll be particularly interested in the invariant $\widehat{HF}$, which assigns to a 3-manifold M an abelian group $\widehat{HF}(M)$ based on a Heegaard diagram for M; indeed, it is shown in [10] that the group $\widehat{HF}(M)$ is independent of the Heegaard diagram used and thus is an invariant of M. Given a knot $K \subset S^3$, we'll be concerned in particular with $\widehat{HF}(\Sigma(K)\#(S^2 \times S^1))$ (and $\widehat{HF}(\Sigma(K))$ in a reduced version of our construction), where $\Sigma(K)$ is the two-fold cover of the sphere S^3 branched along the knot K. The Heegaard Floer homology of branched double-covers was studied in [11], in which Ozsváth and Szabó showed a spectral sequence from the reduced Khovanov homology group $\widetilde{Kh}(-K;\mathbb{Z}/2\mathbb{Z})$ to the group $\widehat{HF}(\Sigma(K);\mathbb{Z}/2\mathbb{Z})$, where $-K$ denotes the mirror of K.

Given a presentation of a knot $K \subset S^3$ as the braid closure of a braid b, Seidel and Smith introduced in [17] the symplectic Khovanov cohomology group $Kh_{symp}(b)$, which is defined by taking the Lagrangian Floer cohomology of two Lagrangian submanifolds inside an affine variety. Clearly there may be different braids which have isotopic braid closures. However, Seidel and Smith proved in [17] that Kh_{symp} is a knot invariant.

Further, by studying the fixed-point sets of an involution on the variety, Seidel and Smith further define in [18] the fixed-point symplectic Khovanov cohomology group $Kh_{symp,inv}(b)$ for a braid b. Via the choice of a particular holomorphic volume form, one obtains gradings (in the sense of [16]) on the totally-real submanifolds $\mathcal{T}$ and $\mathcal{T}'$ used to define $Kh_{symp,inv}(b)$; the gradings on these submanifolds induce an absolute $\mathbb{Z}$-valued Maslov grading $\widetilde{R}$ on the set $\mathcal{T} \cap \mathcal{T}'$.

We'll consider braids in B_{2n}, the braid group on $2n$ strands (where $n \in \mathbb{N}$), and obtain knot diagrams by taking plat closures. Although Seidel and Smith [17],[18] and Manolescu [7] considered braid closures instead, our convention will be chosen for computational reasons (note that Waldron illustrated in [19] that Kh_{symp} can be defined for bridge diagrams coming from such plat closures).

We'll recall the definition for the set $\mathcal{G}$ of **Bigelow generators**, unordered n-tuples of distinct intersection points in a **fork diagram** obtained from the braid b. Following [2] and [7], we'll then define functions $Q, P, T : \mathcal{G} \to \mathbb{Z}$ which can be computed from this diagram in an elementary fashion.

In [7], Manolescu used the fork diagram to give a description of the group $Kh_{symp,inv}(b)$, and in particular showed a one-to-one correspondence between $\mathcal{G}$ and a set of generators for the Seidel-Smith cochain complex. In this context, one can view the totally real submanifolds $\mathcal{T}$ and $\mathcal{T}'$ as admissible Heegaard tori for the manifold $\Sigma(K)\#(S^2 \times S^1)$. Thus the set $\mathcal{G}$ is also in one-to-one correspondence with a set of generators for the chain group $\widehat{CF}(\Sigma(K)\#(S^2 \times S^1))$. This identification provides a function $\widetilde{R} : \mathcal{G} \to \mathbb{Z}$, and following [7] we have that

$$\widetilde{R} = T - Q + P.$$

The function R is obtained from $\widetilde{R}$ by a rational shift s_R which depends on some properties of the braid $b \in B_{2n}$ and the knot diagram D which is its plat closure. Let $e(b)$ be the signed count of braid generators in the word b and let $w(D)$ be the writhe of the diagram D for K given by the plat closure of b. Then define

$$R = \widetilde{R} + s_R(b, D), \quad \text{where} \quad s_R(b, D) = \frac{e(b) - w(D) - 2n}{4}.$$

Furthermore, $\mathfrak{s} \in \mathrm{Spin}^c(M)$ torsion, Ozsváth and Szabó used surgery cobordisms to define an absolute $\mathbb{Q}$-valued grading $\widetilde{gr}$ on the subcomplex $\widehat{CF}(M, \mathfrak{s})$ which is an absolute lift of the relative Maslov $\mathbb{Z}$-grading. Then for torsion $\mathfrak{s}$, define the filtration ρ on the Heegaard Floer chain complex $\widehat{CF}(\Sigma(K)\#(S^2 \times S^1), \mathfrak{s})$ by

$$\rho = R - \widetilde{gr}.$$

Two braids with isotopic plat closures can be connected via a finite sequence of Birman moves [3], which in turn induce sequences of isotopies, handleslides, and stabilizations (and associated chain homotopy equivalences on the Heegaard Floer complexes). We will prove the following theorem about the filtration ρ in Section 5.2:

Theorem 1. *Let the braids $b \in B_{2n}$ and $b' \in B_{2m}$ have plat closures which are diagrams for the knot K. Let $\mathcal{H}$ and $\mathcal{H}'$ be the pointed Heegaard diagrams for $\Sigma(K)\#(S^2 \times S^1)$ induced by b and b',respectively, in the sense of Proposition 21 below. Let $\mathfrak{s} \in Spin^c(\Sigma(K)\#(S^2 \times S^1))$ be torsion. Then the ρ-filtered chain complexes*

$$\widehat{CF}(\mathcal{H}, \mathfrak{s}) \quad \textit{and} \quad \widehat{CF}(\mathcal{H}', \mathfrak{s})$$

have the same filtered chain homotopy type.

More concisely, we can state the following:

Corollary 2. *For each torsion $\mathfrak{s} \in Spin^c(\Sigma(K)\#(S^2 \times S^1))$, the ρ-filtered chain homotopy type of the complex $\widehat{CF}(\Sigma(K)\#(S^2 \times S^1), \mathfrak{s})$ is an invariant of K.*

In a standard way, the filtration ρ provides a spectral sequence (whose pages we'll denote by E_k) computing the group $\widehat{HF}(\Sigma(K)\#(S^2 \times S^1))$. Furthermore, the page E_1 is isomorphic to the subgroup of $Kh_{symp,inv}(b)$ obtained by taking cohomology of the subcomplex whose generators

correspond to generators of $\widehat{CF}$ in the torsion Spin^c structures on $\Sigma(K)\#(S^2\times S^1)$. Seidel and Smith proved in [18] that $Kh_{symp,inv}$ is a knot invariant, and so the the factor corresponding to E_1 is also. Because higher pages are determined by the filtered chain homotopy type of E_0, Corollary 2 implies the following.

Corollary 3. *For $k \geq 1$, the page E_k is a knot invariant.*

Under certain degeneracy conditions of the spectral sequence, the function R in fact provides a homological grading on Heegaard Floer theory. We say that a knot K is **$\boldsymbol{\rho}$-degenerate** if the spectral sequence collapses at E_1 and the induced filtration ρ on E_∞ is constant on each nontrivial factor $\widehat{HF}(\Sigma(K)\#(S^2\times S^1),\mathfrak{s})$. The following is an easy consequence of the definitions.

Proposition 4. *Let $K\subset S^3$ be a knot. Then the following are equivalent:*

(i) K is ρ-degenerate.

(ii) The filtration R is a grading and lifts the relative Maslov $\mathbb{Z}$-grading on each nontrivial factor $\widehat{HF}(\Sigma(K)\#(S^2\times S^1),\mathfrak{s})$.

Moreover, the grading R is a knot invariant when the above hold.

2 Topological preliminaries

In [10], Ozsváth and Szabó define the Heegaard Floer homology group $\widehat{HF}(M)$ associated to a connected, closed, oriented 3-manifold M. A genus-g Heegaard splitting for such a manifold can be described via a **pointed Heegaard diagram** $\mathcal{H}=(\Sigma;\boldsymbol{\alpha};\boldsymbol{\beta};z)$, where Σ is the splitting surface, $\boldsymbol{\alpha}$ and $\boldsymbol{\beta}$ are g-tuples of attaching curves for the handlebodies, and $z\in(\Sigma-\cup\alpha_i-\cup\beta_i)$. The group $\widehat{HF}(M)$ is the Lagrangian Floer of the tori $\mathbb{T}_{\boldsymbol{\alpha}}$ and $\mathbb{T}_{\boldsymbol{\beta}}$ lying inside of the symplectic manifold $Sym^g(\Sigma)$.

Recall that there is a function

$$\mathfrak{s}_z : \mathbb{T}_{\boldsymbol{\alpha}}\cap\mathbb{T}_{\boldsymbol{\beta}} \longrightarrow \text{Spin}^c(M)$$

partitioning $\mathbb{T}_{\boldsymbol{\alpha}}\cap\mathbb{T}_{\boldsymbol{\beta}}$ into equivalence classes $\mathfrak{U}_{\mathfrak{s}}$. This function induces decompositions

$$\widehat{CF}(\mathcal{H}) = \bigoplus_{\mathfrak{s}\in\text{Spin}^c(M)} \widehat{CF}(\mathcal{H},\mathfrak{s}) \quad\text{and}\quad \widehat{HF}(M) = \bigoplus_{\mathfrak{s}\in\text{Spin}^c(M)} \widehat{HF}(M,\mathfrak{s}).$$

For each $\mathfrak{s}\in\text{Spin}^c(M)$ the chain complex $\widehat{CF}(M,\mathfrak{s})$ carries a relative grading gr defined via the Maslov index. For $\mathfrak{s}\in\text{Spin}^c(M)$ torsion, Ozsváth and Szabó use surgery cobordisms to construct in [12] an absolute $\mathbb{Q}$-valued grading $\widetilde{gr}$ on $\mathfrak{U}_{\mathfrak{s}}$ which lifts the relative grading in the following sense: if $\mathbf{x},\mathbf{y}\in\mathfrak{U}_{\mathfrak{s}}$, then

$$\widetilde{gr}(\mathbf{x})-\widetilde{gr}(\mathbf{y}) = gr(\mathbf{x},\mathbf{y}).$$

Whenever $b_1(M)=0$, all Spin^c structures on M are torsion and so the group $\widehat{HF}(M)$ can be absolutely graded via $\widetilde{gr}$. In particular, this holds for $M=\Sigma(K)$ for a knot $K\subset S^3$. However, although Spin$^c(\Sigma(K)\#(S^2\times S^1))$ contains non-torsion elements, the group $\widehat{HF}(\Sigma(K)\#(S^2\times S^1),\mathfrak{s})$ is nontrivial only if $\mathfrak{s}$ is torsion.

2.1 3-gon chain maps and 4-gon homotopies

Remark 5. There can be some ambiguity surrounding terms like "triangle" and "quadrilateral", in particular when distinguishing between the polygons in the symmetric product $Sym^g(\Sigma)$ and the regions which are their shadows in the surface Σ. We'll follow Sarkar's convention in [14] in using neither of these words. The Whitney polygons in symmetric products will be referred to as **n-gons** and regions in surfaces will be referred to as **n-sided regions**.

In [10] and [12], maps between Floer homologies are constructed by counting pseudo-holomorphic 3-gons in a certain equivalence class. We review these ideas below.

First recall the notion of a **pointed Heegaard triple-diagram** $(\Sigma; \boldsymbol{\alpha}; \boldsymbol{\beta}; \boldsymbol{\gamma}; z)$, where Σ is an oriented two-manifold of genus g, $\boldsymbol{\alpha}$, $\boldsymbol{\beta}$, and $\boldsymbol{\gamma}$ are complete g-tuples of attaching circles for handlebodies U_α, U_β, and U_γ, respectively, and $z \in (\Sigma - \cup\alpha_i - \cup\beta_i - \cup\gamma_i)$. We then have pointed Heegaard diagrams $\mathcal{H}_{\boldsymbol{\alpha\beta}} = (\Sigma; \boldsymbol{\alpha}; \boldsymbol{\beta}; z)$, $\mathcal{H}_{\boldsymbol{\beta\gamma}}\,(\Sigma; \boldsymbol{\beta}; \boldsymbol{\gamma}; z)$, and $\mathcal{H}_{\boldsymbol{\alpha\gamma}} = (\Sigma; \boldsymbol{\alpha}; \boldsymbol{\gamma}; z)$, depicting manifolds $Y_{\boldsymbol{\alpha\beta}}$, $Y_{\boldsymbol{\beta\gamma}}$, and $Y_{\boldsymbol{\alpha\gamma}}$, respectively.

Under some admissibility conditions discussed in [10], there is a chain map

$$\widehat{f}_{\alpha\beta\gamma} : \widehat{CF}(\mathcal{H}_{\boldsymbol{\alpha\beta}}) \otimes \widehat{CF}(\mathcal{H}_{\boldsymbol{\beta\gamma}}) \to \widehat{CF}(\mathcal{H}_{\boldsymbol{\alpha\gamma}})$$

given by the formula

$$\widehat{f}_{\alpha\beta\gamma}(\mathbf{x} \otimes \mathbf{y}) = \sum_{\mathbf{w} \in \mathbb{T}_{\boldsymbol{\alpha}} \cap \mathbb{T}_{\boldsymbol{\gamma}}} \left(\sum_{\{\psi \in \pi_2(\mathbf{x},\mathbf{y},\mathbf{w}) | \mu(\psi)=0, n_z(\psi)=0\}} (\#\mathcal{M}(\psi)) \right) \mathbf{w}$$

with induced map $\widehat{F}_{\alpha\beta\gamma}$ on homology.

There is an analogous notion of a **pointed Heegaard quadruple-diagram** $(\Sigma; \boldsymbol{\alpha}; \boldsymbol{\beta}; \boldsymbol{\gamma}; \boldsymbol{\delta}; z)$. Then under admissibility conditions analogous to those for the 3-gon maps, one can define a map

$$\widehat{h}_{\alpha\beta\gamma\delta} : \widehat{CF}(\mathcal{H}_{\boldsymbol{\alpha\beta}}) \otimes \widehat{CF}(\mathcal{H}_{\boldsymbol{\beta\gamma}}) \otimes \widehat{CF}(\mathcal{H}_{\boldsymbol{\gamma\delta}}) \to \widehat{CF}(\mathcal{H}_{\boldsymbol{\alpha\delta}})$$

by the formula

$$\widehat{h}_{\alpha\beta\gamma\delta}(\mathbf{x} \otimes \mathbf{y} \otimes \mathbf{w}) = \sum_{\mathbf{z} \in \mathbb{T}_{\boldsymbol{\alpha}} \cap \mathbb{T}_{\boldsymbol{\delta}}} \left(\sum_{\{\psi \in \pi_2(\mathbf{x},\mathbf{y},\mathbf{w},\mathbf{z}) | \mu(\psi)=-1, n_z(\psi)=0\}} (\#\mathcal{M}(\psi)) \right) \mathbf{z}$$

A 4-gon map actually provides a chain homotopy between two compositions of 3-gon maps:

Theorem 6 ([10])**.** *Let $(\Sigma; \boldsymbol{\alpha}; \boldsymbol{\beta}; \boldsymbol{\gamma}; \boldsymbol{\delta}; z)$ be an admissible pointed Heegaard quadruple-diagram. Then for $\xi \in \widehat{CF}(\mathcal{H}_{\boldsymbol{\alpha\beta}})$, $\eta \in \widehat{CF}(\mathcal{H}_{\boldsymbol{\beta\gamma}})$, and $\zeta \in \widehat{CF}(\mathcal{H}_{\boldsymbol{\gamma\delta}})$,*

$$\partial\widehat{h}_{\alpha\beta\gamma\delta}(\xi \otimes \eta \otimes \zeta) + \widehat{h}_{\alpha\beta\gamma\delta}(\partial(\xi \otimes \eta \otimes \zeta)) = \widehat{f}_{\alpha\gamma\delta}(\widehat{f}_{\alpha\beta\gamma}(\xi \otimes \eta) \otimes \zeta) - \widehat{f}_{\alpha\beta\delta}(\xi \otimes \widehat{f}_{\beta\gamma\delta}(\eta \otimes \zeta))$$

2.1.1 Some index-zero 3-gon classes

We're interested in 3-gon classes of Maslov index zero. To calculate index, we'll follow Sarkar's work in [14] on Whitney n-gons, which we'll review here. Some labeling conventions have been modified to fit our notation, and we'll specialize to the $n = 3$ case for this discussion.

Let $(\Sigma; \boldsymbol{\alpha}; \boldsymbol{\beta}; \boldsymbol{\gamma}; z)$ be a pointed Heegaard diagram, and let ψ be a 3-gon class connecting $\mathbf{x}$, $\mathbf{y}$, and $\mathbf{w}$ as defined above. Denote by $a(\psi)$, $b(\psi)$, and $c(\psi)$ the boundaries $\partial\mathcal{D}(\psi)|_\alpha$, $\partial\mathcal{D}(\psi)|_\beta$, and $\partial\mathcal{D}(\psi)|_\gamma$, respectively.

Now given some 1-chains a supported on α and b supported on β, Sarkar defines the number $b.a$ as follows. Assuming some orientation on the α and β circles and on Σ, we have four well-defined directions in which we can translate b so that no endpoint of a lies on the translate b' and no endpoint of b' lies on a. These can be thought of as 'northeast", "northwest", "southeast", and "southwest". After a small translation in some direction, we can calculate the intersection number of b' with a. Then $b.a$ is defined to be the average of these numbers over the four possible translation directions.

Some element $\mathbf{x} \in \mathbb{T}_{\boldsymbol{\alpha}} \cap \mathbb{T}_{\boldsymbol{\beta}}$ is a g-tuple $(x_1, x_2, \ldots, x_g)$. Define the number $\mu_x(\psi) = \sum \mu_{x_i}(\psi)$, where $\mu_{x_i}(\psi)$ is the average of the local coefficients of the 2-chain $\mathcal{D}(\psi)$ over the four quadrants around $x_i \in \Sigma$.

The Euler measure of $\mathcal{D}(\psi)$ will be denoted by $e(\psi)$. The Euler measure is additive, and it is enough for our purposes to know that the measure of an n-sided region is $(1 - n/4)$.

Equipped with these concepts, we present the following formula of Sarkar:

Theorem 7 ([14])**.** *Let $(\Sigma; \boldsymbol{\alpha}; \boldsymbol{\beta}; \boldsymbol{\gamma}; z)$ be a pointed Heegaard diagram, and let ψ be a 2-chain on Σ representing a 3-gon class connecting $\mathbf{x}$, $\mathbf{y}$, and $\mathbf{w}$. Then the Maslov index $\mu(\psi)$ satisfies the formula*

$$\mu(\psi) = e(\psi) + \mu_{\mathbf{x}}(\psi) + \mu_{\mathbf{y}}(\psi) + a(\psi).c(\psi) - g/2. \tag{2.1}$$

Here we'll discuss two types of 3-gon classes in $Sym^g(\Sigma)$.

A 3-gon ψ of the first type has domain $\mathcal{D}(\psi)$ given by the sum of g disjoint 3-sided regions, each with coefficient $+1$. A 3-gon ψ of the second type has domain $\mathcal{D}(\psi')$ given by the sum of $(g-1)$ disjoint regions, consisting of $(g-2)$ 3-sided regions and a single 6-sided region with one angle larger than π, each with coefficient $+1$. These types can be seen in Figures 1 and 2, respectively. Components of $\boldsymbol{\alpha}$, $\boldsymbol{\beta}$, and $\boldsymbol{\gamma}$ are solid, dashed, and dotted arcs, respectively. Components of $\mathbf{x}$, $\mathbf{y}$, and $\mathbf{w}$ are dark gray, white, and light gray dots, respectively.

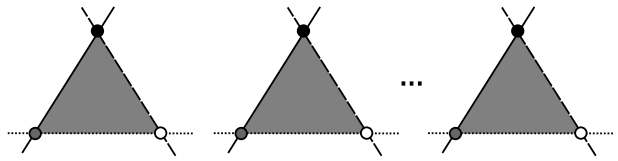

Figure 1: The domain $\mathcal{D}(\psi)$ for a type I 3-gon ψ

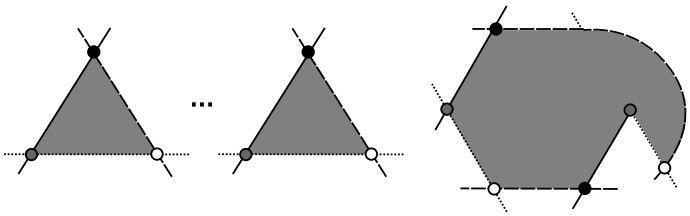

Figure 2: The domain $\mathcal{D}(\psi)$ for a type II 3-gon ψ

The reader can verify that $\mu(\psi) = 0$ in either case (in the second, it will help to split the obtuse hexagonal component of the domain as seen in Figure 3).

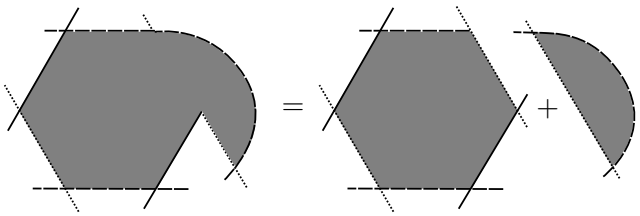

Figure 3: Decomposing the obtuse 6-sided component of $\mathcal{D}(\psi)$.

2.1.2 3-gons and 4-gons in Heegaard moves

Now let $Y_{\boldsymbol{\beta\gamma}} = \#_g(S^1 \times S^2)$. Denote by $\boldsymbol{\theta}_{\boldsymbol{\beta\gamma}} \in \mathbb{T}_{\boldsymbol{\beta}} \cap \mathbb{T}_{\boldsymbol{\gamma}}$ the intersection point representing the top-degree homology class in $\widehat{HF}(Y_{\boldsymbol{\beta\gamma}})$. Based on the orientation convention of pseudo-holomorphic disks used in the differential, it's easy to choose components of $\boldsymbol{\theta}_{\boldsymbol{\beta\gamma}}$. We then have a well-defined chain map

$$\widehat{f}_{\alpha\beta\gamma}(\cdot \otimes \boldsymbol{\theta}_{\boldsymbol{\beta\gamma}}) : \widehat{CF}(\mathcal{H}_{\boldsymbol{\alpha\beta}}) \to \widehat{CF}(\mathcal{H}_{\boldsymbol{\alpha\gamma}}).$$

Similarly, if $Y_{\boldsymbol{\alpha\beta}} = \#_g(S^1 \times S^2)$, one can obtain a chain map

$$\widehat{f}_{\alpha\beta\gamma}(\boldsymbol{\theta}_{\boldsymbol{\alpha\beta}} \otimes \cdot) : \widehat{CF}(\mathcal{H}_{\boldsymbol{\beta\gamma}}) \to \widehat{CF}(\mathcal{H}_{\boldsymbol{\alpha\gamma}}).$$

We'll use this construction in the contexts of isotopies and handleslides among the $\boldsymbol{\beta}$ circles. Note that in the original proof of invariance in [10], isotopies weren't treated in terms of a chain map which counts pseudo-holomorphic 3-gons. Lipshitz proves in Proposition 11.4 from [6] that this can be done.

Consider a Heegaard triple-diagram $\left(\Sigma; \boldsymbol{\alpha}; \boldsymbol{\beta}; \boldsymbol{\beta}'\right)$. For the isotopy case, we'll have that the $\boldsymbol{\beta}'$ circles and $\boldsymbol{\beta}$ circles differ by isotopies with β_i intersecting β_i' transversely in exactly two points for each i (we'll say that β_i' and β_i differ by an **admissible isotopy**). For a handleslide, let β_1' be a circle such that β_1, β_2, and β_1' bound an embedded pair of pants and such that β_1' intersects β_1 transversely in two points (an **admissible handleslide**). For $i > 1$, let β_i' be obtained as in the isotopy case. In either case, indeed $Y_{\boldsymbol{\beta\beta'}} = \#^g(S^1 \times S^2)$ and we can acquire the chain map $\widehat{f}_{\alpha\beta\beta'}(\cdot \otimes \boldsymbol{\theta}_{\boldsymbol{\beta\beta'}})$ as mentioned above.

Now let $\widetilde{\boldsymbol{\beta}}$ be a g-tuple of attaching circles such that for each i, $\widetilde{\beta}_i$ and β_i differ by an admissible isotopy. One can then study the Heegaard quadruple-diagram $\left(\Sigma; \boldsymbol{\alpha}; \boldsymbol{\beta}; \boldsymbol{\beta}'; \widetilde{\boldsymbol{\beta}}\right)$. We can identify $Y_{\boldsymbol{\alpha\beta}} = Y_{\boldsymbol{\alpha},\widetilde{\boldsymbol{\beta}}}$ via the nearest-neighbor map $\mathbf{x} \mapsto \widetilde{\mathbf{x}}$, and

$$\widehat{f}_{\boldsymbol{\alpha\beta}\widetilde{\boldsymbol{\beta}}}\left(\mathbf{x} \otimes \widehat{f}_{\boldsymbol{\beta\beta'}\widetilde{\boldsymbol{\beta}}}\left(\boldsymbol{\theta}_{\boldsymbol{\beta\beta'}} \otimes \boldsymbol{\theta}_{\boldsymbol{\beta}'\widetilde{\boldsymbol{\beta}}}\right)\right) = \widehat{f}_{\boldsymbol{\alpha\beta}\widetilde{\boldsymbol{\beta}}}\left(\mathbf{x} \otimes \boldsymbol{\theta}_{\boldsymbol{\beta}\widetilde{\boldsymbol{\beta}}}\right) = \widetilde{\mathbf{x}} \quad \text{for all} \quad \mathbf{x} \in \mathbb{T}_{\boldsymbol{\alpha}} \cap \mathbb{T}_{\boldsymbol{\beta}}.$$

Then by Theorem 6, we have that

$$\begin{aligned}&\widehat{f}_{\boldsymbol{\alpha\beta'}\widetilde{\boldsymbol{\beta}}}\left(\widehat{f}_{\boldsymbol{\alpha\beta\beta'}}\left(\mathbf{x} \otimes \boldsymbol{\theta}_{\boldsymbol{\beta\beta'}}\right) \otimes \boldsymbol{\theta}_{\boldsymbol{\beta}'\widetilde{\boldsymbol{\beta}}}\right) - id_{\widehat{CF}(Y_{\boldsymbol{\alpha\beta}})} = \\ &\widehat{\partial}\left(\widehat{h}_{\boldsymbol{\alpha\beta\beta'}\widetilde{\boldsymbol{\beta}}}\left(\cdot \otimes \boldsymbol{\theta}_{\boldsymbol{\beta\beta'}} \otimes \boldsymbol{\theta}_{\boldsymbol{\beta}'\widetilde{\boldsymbol{\beta}}}\right)\right) + \widehat{h}_{\boldsymbol{\alpha\beta\beta'}\widetilde{\boldsymbol{\beta}}}\left(\widehat{\partial}\left(\cdot \otimes \boldsymbol{\theta}_{\boldsymbol{\beta\beta'}} \otimes \boldsymbol{\theta}_{\boldsymbol{\beta}'\widetilde{\boldsymbol{\beta}}}\right)\right).\end{aligned}$$

Similarly, by letting $\widetilde{\boldsymbol{\beta}'}$ be admissibly isotopic translates of $\boldsymbol{\beta}'$ and studying the quadruple-diagram

$\left(\Sigma;\boldsymbol{\alpha};\boldsymbol{\beta}';\boldsymbol{\beta};\widetilde{\boldsymbol{\beta}}'\right)$, one finds that

$$\widehat{f}_{\boldsymbol{\alpha}\boldsymbol{\beta}'\widetilde{\boldsymbol{\beta}}'}\left(\widehat{f}_{\boldsymbol{\alpha}\boldsymbol{\beta}'\boldsymbol{\beta}}\left(\mathbf{x}\otimes\boldsymbol{\theta}_{\boldsymbol{\beta}'\boldsymbol{\beta}}\right)\otimes\boldsymbol{\theta}_{\boldsymbol{\beta}\widetilde{\boldsymbol{\beta}}'}\right)-id_{\widehat{CF}(Y_{\boldsymbol{\alpha}\boldsymbol{\beta}'})}=$$
$$\widehat{\partial}\left(\widehat{h}_{\boldsymbol{\alpha}\boldsymbol{\beta}'\boldsymbol{\beta}\widetilde{\boldsymbol{\beta}}'}\left(\cdot\otimes\boldsymbol{\theta}_{\boldsymbol{\beta}'\boldsymbol{\beta}}\otimes\boldsymbol{\theta}_{\boldsymbol{\beta}\widetilde{\boldsymbol{\beta}}'}\right)\right)+\widehat{h}_{\boldsymbol{\alpha}\boldsymbol{\beta}'\boldsymbol{\beta}\widetilde{\boldsymbol{\beta}}'}\left(\widehat{\partial}\left(\cdot\otimes\boldsymbol{\theta}_{\boldsymbol{\beta}'\boldsymbol{\beta}}\otimes\boldsymbol{\theta}_{\boldsymbol{\beta}\widetilde{\boldsymbol{\beta}}'}\right)\right).$$

Therefore, we see that when $\boldsymbol{\beta}'$ and $\boldsymbol{\beta}$ are related by an isotopy or a handleslide, the chain map $\widehat{f}_{\alpha\beta\beta'}(\cdot\otimes\boldsymbol{\theta}_{\boldsymbol{\beta}\boldsymbol{\beta}'})$ is a chain homotopy equivalence with homotopy inverse given by $\widehat{f}_{\alpha\beta'\beta}(\cdot\otimes\boldsymbol{\theta}_{\boldsymbol{\beta}'\boldsymbol{\beta}})$.

Remark 8. When $\boldsymbol{\alpha}'$ and $\boldsymbol{\alpha}$ differ by an admissible isotopy or admissible handleslide, one can define the chain maps $\widehat{f}_{\boldsymbol{\alpha}',\boldsymbol{\alpha},\boldsymbol{\beta}}(\boldsymbol{\theta}_{\boldsymbol{\alpha}'\boldsymbol{\alpha}}\otimes\cdot)$ and $\widehat{f}_{\boldsymbol{\alpha},\boldsymbol{\alpha}',\boldsymbol{\beta}}(\boldsymbol{\theta}_{\boldsymbol{\alpha}'\boldsymbol{\alpha}}\otimes\cdot)$ using the Heegaard triple-diagrams $(\Sigma;\boldsymbol{\alpha}';\boldsymbol{\alpha};\boldsymbol{\beta})$ and $(\Sigma;\boldsymbol{\alpha};\boldsymbol{\alpha}';\boldsymbol{\beta})$. These two maps are chain homtopy inverses to one another, and the associated chain homotopies

$$\widehat{h}_{\widetilde{\boldsymbol{\alpha}}\boldsymbol{\alpha}'\boldsymbol{\alpha}\boldsymbol{\beta}}\left(\boldsymbol{\theta}_{\widetilde{\boldsymbol{\alpha}}\boldsymbol{\alpha}'}\otimes\boldsymbol{\theta}_{\boldsymbol{\alpha}'\boldsymbol{\alpha}}\otimes\cdot\right)\quad\text{and}\quad\widehat{h}_{\widetilde{\boldsymbol{\alpha}}'\boldsymbol{\alpha}\boldsymbol{\alpha}'\boldsymbol{\beta}}\left(\boldsymbol{\theta}_{\widetilde{\boldsymbol{\alpha}}'\boldsymbol{\alpha}}\otimes\boldsymbol{\theta}_{\boldsymbol{\alpha}\boldsymbol{\alpha}'}\otimes\cdot\right)$$

can be defined using the quadruple diagrams $(\Sigma;\widetilde{\boldsymbol{\alpha}};\boldsymbol{\alpha}';\boldsymbol{\alpha};\boldsymbol{\beta})$ and $\left(\Sigma;\widetilde{\boldsymbol{\alpha}}';\boldsymbol{\alpha};\boldsymbol{\alpha}';\boldsymbol{\beta}\right)$, respectively.

2.2 Periodic domains

Recall that a periodic domain in a pointed Heegaard diagram $(\Sigma;\boldsymbol{\alpha};\boldsymbol{\beta};z)$ is a domain avoiding the basepoint z whose boundary is a sum of the $\boldsymbol{\alpha}$ and $\boldsymbol{\beta}$ circles. Denote by $\Pi_{\boldsymbol{\alpha}\boldsymbol{\beta}}\subset H_2\left(\Sigma;\mathbb{Z}\right)$ the group of such periodic domains and let $S_{\boldsymbol{\alpha}\boldsymbol{\beta}}=S_{\boldsymbol{\alpha}}+S_{\boldsymbol{\beta}}\subset H_1\left(\Sigma;\mathbb{Z}\right)$ be the span of the $\boldsymbol{\alpha}$ and $\boldsymbol{\beta}$ circles.

One can define analogous notions of triply- and quadruply-periodic domains in Heegaard triple-diagrams and quadruple-diagrams.

In [8], it is shown that if $(\Sigma;\boldsymbol{\alpha};\boldsymbol{\beta};z)$ is a pointed Heegaard diagram, then $\Pi_{\boldsymbol{\alpha}\boldsymbol{\beta}}$ is a free Abelian group of rank $2g-\mathrm{rank}(S_{\boldsymbol{\alpha}\boldsymbol{\beta}})$. It can be shown in a completely analogous way that for a triple-diagram (respectively quadruple-diagram), the group $\Pi_{\boldsymbol{\alpha}\boldsymbol{\beta}\boldsymbol{\gamma}}$ (respectively $\Pi_{\boldsymbol{\alpha}\boldsymbol{\beta}\boldsymbol{\gamma}\boldsymbol{\delta}}$) is free Abelian of rank $3g-\mathrm{rank}(S_{\boldsymbol{\alpha}\boldsymbol{\beta}\boldsymbol{\gamma}})$ (respectively $4g-\mathrm{rank}(S_{\boldsymbol{\alpha}\boldsymbol{\beta}\boldsymbol{\gamma}\boldsymbol{\delta}})$). One should note that because we don't permit periodic domains in a pointed Heegaard diagram to intersect the basepoint, our ranks are 1 lower than those stated in [8].

Let $\boldsymbol{\alpha}$ and $\boldsymbol{\beta}$ be two g-tuples of attaching circles on a genus-g surface Σ such that $\boldsymbol{\beta}$ is obtained from $\boldsymbol{\alpha}$ via admissible isotopies. Then for each i, the circles α_i and β_i are separated by two thin 2-sided regions, and we denote by $\mathcal{D}_i^{\boldsymbol{\alpha}\boldsymbol{\beta}}$ the periodic domain which is their difference.

Now instead $\boldsymbol{\alpha}$ and $\boldsymbol{\beta}$ be two g-tuples of attaching circles on a genus-g surface Σ such that $\boldsymbol{\beta}$ is obtained from $\boldsymbol{\alpha}$ via an admissible handleslide of α_1 over α_2.

For $i>1$, the circles α_i and β_i are separated by two thin 2-sided regions, and we denote by $\mathcal{D}_i^{\boldsymbol{\alpha}\boldsymbol{\beta}}$ the periodic domain which is their difference. The circles α_1 and β_1 are separated by a thin 2-sided region, and we denote by $\mathcal{D}_1^{\boldsymbol{\alpha}\boldsymbol{\beta}}$ the periodic domain which is the difference between this region and the annulus bounded by α_1, α_2, and β_1.

The following facts are exercises in linear algebra:

Proposition 9. *Let $(\Sigma;\boldsymbol{\alpha};\boldsymbol{\beta};\boldsymbol{\gamma};z)$ be a Heegaard triple-diagram such that $Y_{\boldsymbol{\alpha}\boldsymbol{\beta}}$ is a rational-homology sphere and $\boldsymbol{\gamma}$ is obtained from $\boldsymbol{\beta}$ via an isotopy or handleslide. Then the set $\{\mathcal{D}_1^{\boldsymbol{\beta}\boldsymbol{\gamma}},\ldots,\mathcal{D}_g^{\boldsymbol{\beta}\boldsymbol{\gamma}}\}$ is a generating set for the group $\Pi_{\boldsymbol{\alpha}\boldsymbol{\beta}\boldsymbol{\gamma}}$.*

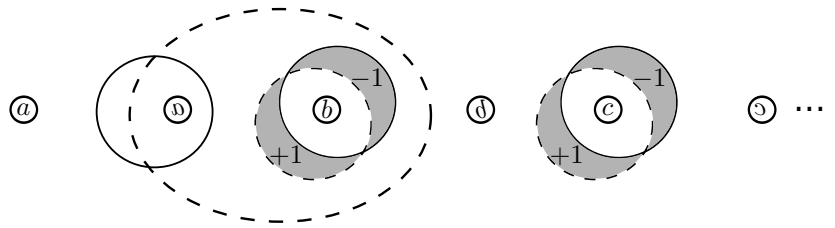

(a) The handleslide domains $\mathcal{D}_i^{\boldsymbol{\alpha\beta}}$ for $i > 1$.

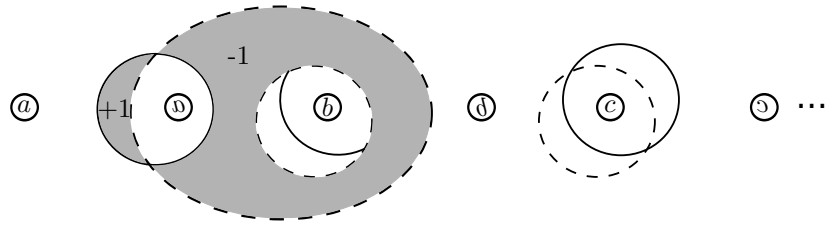

(b) The handleslide domain $\mathcal{D}_1^{\boldsymbol{\alpha\beta}}$.

Figure 4: The periodic domains $\mathcal{D}_i^{\boldsymbol{\alpha\beta}}$ for the handleslide of α_1 over α_2. The $\boldsymbol{\alpha}$ circles are solid and the $\boldsymbol{\beta}$ circles are dashed. The domains of interest are shaded and local coefficients are labelled.

Proposition 10. *Let $(\Sigma; \boldsymbol{\alpha}; \boldsymbol{\beta}; \boldsymbol{\gamma}; \boldsymbol{\delta}; z)$ be a Heegaard quadruple-diagram such that $Y_{\boldsymbol{\alpha\beta}}$ is a rational-homology sphere, $\boldsymbol{\gamma}$ is obtained from $\boldsymbol{\beta}$ via some isotopy or handleslide, and $\boldsymbol{\delta}$ is obtained from $\boldsymbol{\alpha}$ via a small isotopy. Then the set $\{\mathcal{D}_1^{\boldsymbol{\beta\gamma}}, \dots, \mathcal{D}_g^{\boldsymbol{\beta\gamma}}\} \cup \{\mathcal{D}_1^{\boldsymbol{\alpha\delta}}, \dots, \mathcal{D}_g^{\boldsymbol{\alpha\delta}}\}$ is a generating set for the group $\Pi_{\boldsymbol{\alpha\beta\gamma\delta}}$.*

2.3 Filtrations and spectral sequences

Let $(\mathcal{C}, \partial)$ be a chain complex generated by $\{x_i\}_{i=1}^n$ and equipped with a filtration grading $f : \{x_i\} \to \mathbb{Z}$. We can view the filtration as the nested family of subcomplexes $\{\mathcal{F}_k\}_{k\in\mathbb{Z}}$, with

$$\mathcal{F}_k = \text{span}\{x_i : f(x_i) \leq k\}.$$

Definition 11. Let $(\mathcal{C}, \partial)$ and $(\mathcal{C}', \partial')$ be chain complexes with filtrations $\{\mathcal{F}_k\}$ and $\{\mathcal{F}'_k\}$.

(a) A chain map $F : (\mathcal{C}, \partial) \to (\mathcal{C}', \partial')$ is called a **filtered chain map** if for all k, $F(\mathcal{F}_k) \subset \mathcal{F}'_k$.

(b) Let $H : (\mathcal{C}, \partial) \to (\mathcal{C}', \partial')$ be a chain homotopy connecting two maps $F, G : (\mathcal{C}, \partial) \to (\mathcal{C}', \partial')$. We call H a **filtered chain homotopy** if for all k, $H(\mathcal{F}_k) \subset \mathcal{F}'_{k+1}$.

(c) Let $F : (\mathcal{C}, \partial) \to (\mathcal{C}', \partial')$ be a chain homotopy equivalence with homotopy inverse map $G : (\mathcal{C}', \partial') \to (\mathcal{C}, \partial)$ and associated homotopies $H : (\mathcal{C}, \partial) \to (\mathcal{C}, \partial)$ from $G \circ F$ to $id_{\mathcal{C}}$ and $H' : (\mathcal{C}', \partial') \to (\mathcal{C}', \partial')$ from $F \circ G$ to $id_{\mathcal{C}'}$. We say that F is a **filtered chain homotopy equivalence** if both F and G are filtered maps and both H and H' are filtered chain homotopies.

Given a filtered chain complex $(\mathcal{C}, \partial)$, one can decompose the differential ∂ with respect to the filtration grading by letting

$$\partial(x) = \partial_0(x) + \partial_1(x) + \partial_2(x) + \dots \quad \text{where} \quad \partial_m(x) = \sum_{f(x_j)=f(x)-m} A_{m,j} x_j.$$

Now $\mathcal{C}_0 = (\mathcal{C}, \partial_0)$ is a chain complex, and $\mathcal{C}_m = (H_*(\mathcal{C}_{m-1}, \partial_{m-1}), \partial_m)$ is a chain complex for $m \geq 1$. We refer to the complex $\mathcal{C}_m$ as the E_m-page of the spectral sequence. For $m \geq 1$, the E_m-page is uniquely determined by the filtered chain homotopy type of the original filtered complex $(\mathcal{C}, \partial)$. Notice that since there are finitely many elements in the generating set $\{x_i\}$, then all but finitely many of the ∂_m vanish, and therefore the sequence stabilizes within finitely-many pages. The limit of the sequence of chain complexes (the E_∞-page) is exactly $(H(\mathcal{C}, \partial), 0)$.

3 Braids and the Bigelow picture

Let B_{2n} denote the braid group on $2n$ strands. This group is generated by $\{\sigma_1, \dots, \sigma_{2n-1}\}$, where σ_k denotes a half-twist of the k^{th} strand over the $(k+1)^{st}$ strand. Given a braid $b \in B_{2n}$, we can obtain a diagram of a knot or a link (the **plat closure** of b) by connecting ends of consecutive strands with segments at the top and bottom, as shown in Figure 5.

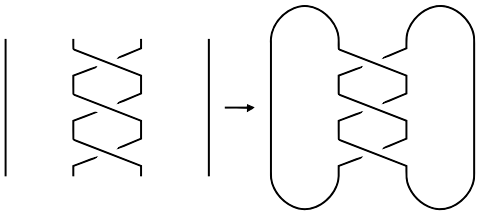

Figure 5: The left-handed trefoil

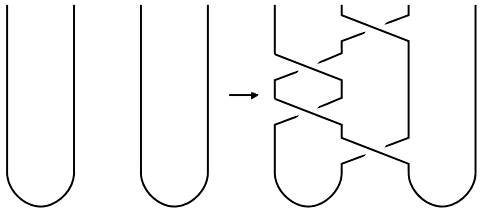

Figure 6: The Birman move $b \mapsto bB$

Any knot K can be presented as the plat closure of an element in B_{2n}. Many distinct braid elements can have isotopic plat closures, but such braids are related.

Definition 12. Let K_{2n} be the subgroup of the braid group B_{2n} generated by $A = \sigma_1$, $B = \sigma_2\sigma_1^2\sigma_2$, and $C_i = \sigma_{2i}\sigma_{2i-1}\sigma_{2i+1}\sigma_{2i}$ for $i = 1, 2, \dots, 2n$.

Theorem 13 (Theorem 1 from [3])**.** *Let $b \in B_{2n}$ and $b' \in B_{2n'}$ be two oriented braids. The braids b and b' have isotopic plat closures if and only if they are related by a finite sequence of the following moves:*

(i) $b \mapsto gbh$ *where* $b \in B_{2n}$ *and* $g, h \in K_{2n}$

(ii) $b \leftrightarrow \sigma_{2n} b$ *where* $b \in B_{2n}$ *and* $\sigma_{2n} b \in B_{2n+2}$

3.1 The Bigelow generators

Let $D_{2n} \subset \mathbb{C}$ denote the unit disk with $2n$ punctures $\mu_1, \dots, \mu_{2n}$ evenly spaced along $\mathbb{R} \cap D$. We can view the braid group B_{2n} as the mapping class group of D_{2n}, where the generator σ_k is a diffeomorphism which is the identity outside of a neighborhood of the k^{th} and $(k+1)^{st}$ punctures

and exchanges these two punctures by a counter-clockwise half-twist. Any braid can be written as a word in the $\sigma_k's$, and we view them as operating on D_{2n} in this way, read from left to right.

Let $b \in B_{2n}$ be an oriented braid on $2n$ strands. We'll establish some terminology, following Bigelow in [2].

Definition 14. Let $D \subset \mathbb{C}$ be the unit disk.

(i) Let the **standard fork diagram** in D_{2n} be a collection of maps

$$\alpha_1, \ldots, \alpha_n : I \to D \quad \text{and} \quad h_1, \ldots, h_n : I \to D$$

called **tine edges** and **handles**, respectively, such that the following hold:

(a) The segments $\alpha_i|_{(0,1)}$ are disjoint embeddings of $(0,1)$ into D_{2n} such that for each k, $\alpha_k(0) = \mu_{2k-1}$, $\alpha_k(1) = \mu_{2k}$, and $\alpha_k(t) \in \mathbb{R}$ for all $t \in I$.

(b) The segments $h_i|_{(0,1)}$ are disjoint embeddings of $(0,1)$ into D_{2n} such that that for each k, $h_k(1) = d_k \in \partial D$, $h_k(0) = m_k$ is the midpoint of the segment α_k, and the segment h_k is vertical.

(ii) Let a **fork diagram for b** be the standard fork diagram along with the compositions $b \circ \alpha_1, \ldots, b \circ \alpha_n$ and $b \circ h_1, \ldots, b \circ h_n$. We'll let $\beta_k = b \circ \alpha_k$.

(iii) Let an **augmented fork diagram for b** be obtained from a fork diagram by replacing each arc β_k with bE_k, where E_k is a figure-eight encircling μ_{2k-1} and μ_{2k}, where E_k is oriented such that it winds counter-clockwise about μ_{2k}.

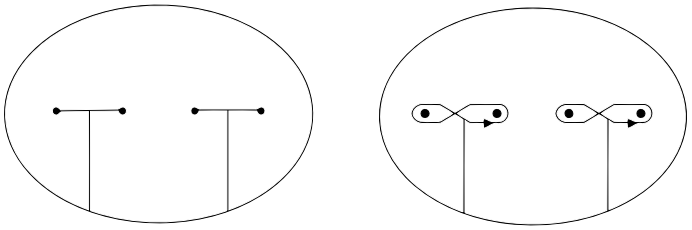

(a) Tine edges α_k (b) Figure-eights E_k

Figure 7: Structures in fork diagrams

The reader should notice that by drawing a picture containing just the α and β arcs and treating the α arcs as undercrossings at each intersection, we get a diagram of the plat closure of b.

We'll define some notation. Let $Conf^n(\mathbb{C})$ denote the configuration space of $\mathbb{C}$, i.e. the set of unordered n-tuples of distinct points in $\mathbb{C}$. Let $\widetilde{\mathcal{Z}}$ be the set of intersections between α and β arcs. Then if τ denotes the set of puncture points, we see that $\tau \subset \widetilde{\mathcal{Z}}$. Then we construct a set $\mathcal{Z}$ by doubling the points in $\widetilde{\mathcal{Z}} - \tau$ by introducing for each $x \in \tau$ one element $e_x \in \mathcal{Z}$ and for each $x \in \widetilde{\mathcal{Z}} - \tau$ two elements $e_x, e_x' \in \mathcal{Z}$. The set $\mathcal{Z}$ can then be seen as the intersections points between α arcs and figure-eights bE_k. We distinguish between e_x and e_x' by requiring that the loop traveling along a figure-eight from e_x to e_x' and back to e_x along an α arc has winding number $+1$ around the puncture point.

Remark 15. Via an abuse of notation, we'll often refer to the points corresponding to $x \in \widetilde{\mathcal{Z}}$ as $x \in \mathcal{Z}$ (if $x \in \tau$) or $x, x' \in \mathcal{Z}$ (if $x \in \widetilde{\mathcal{Z}} - \tau$).

We then define

$$\widetilde{\mathcal{G}} = (\alpha_1 \times \ldots \times \alpha_n) \cap (\beta_1 \times \ldots \times \beta_n) \subset Conf^n(\mathbb{C}),$$

the set of unordered n-tuples of points in $\widetilde{\mathcal{Z}}$ such that no two points are on the same α or β arcs. Similarly, define

$$\mathcal{G} = (\alpha_1 \times \ldots \times \alpha_n) \cap (bE_1 \times \ldots \times bE_n) \subset Conf^n(\mathbb{C}),$$

the set of unordered n-tuples of points in $\mathcal{Z}$ such that no two points are on the same α arcs or figure-eights. The set $\mathcal{G}$ will be referred to as the set of **Bigelow generators** for the diagram.

Remark 16. From this point forward, something of the form $x\mathbf{y}$ will denote an element in $\mathcal{G}$ or $\widetilde{\mathcal{G}}$ such that $x \in \mathcal{Z}$ or $x \in \widetilde{\mathcal{Z}}$ is some component of the n-tuple and $\mathbf{y}$ is the rest of the n-tuple.

3.2 Gradings on the Bigelow generators

We will define some gradings $Q, T, P : \mathcal{G} \to \mathbb{Z}$ based on loops in the configuration space of the disk. Our definitions of Q and T are identical to Bigelow's in [2], while our definition for P is adapted from Manolescu's definition for $\widetilde{P}$ in [7] (in which he used braid closures).

For the sake of concreteness, a sample calculation will accompany the description of the gradings. We'll study the left-handed trefoil knot depicted as the plat closure of $\sigma_2^3 \in B_4$, as seen in Figure 5.

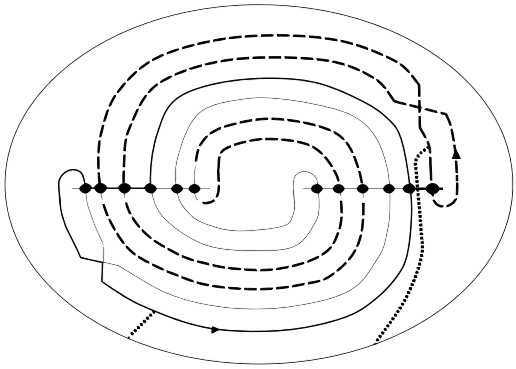

Figure 8: The augmented fork diagram induced by $\sigma_2^3 \in B_4$

Figure 8 depicts the augmented fork diagram for our example. Label the elements of $\mathcal{Z}$ from left to right in the diagram as

$$\mathcal{Z} = \{x_1, s, s', t, t', x_2, x_3, u', u, v', v, x_4\}.$$

One can verify that the set of Bigelow generators is given by

$$\mathcal{G} = \begin{Bmatrix} x_1x_4, & x_1u, & x_1u', & x_2v, & x_2v', & x_2x_3, & sx_3, & s'x_3, & tx_4, \\ t'x_4, & sv, & s'v, & sv', & s'v', & tu, & t'u, & tu', & t'u' \end{Bmatrix}.$$

We'll turn to defining various gradings on the set $\mathcal{G}$. Grading distributions for our trefoil example can be found in Table 1. Figure 9 illustrates how to compute the gradings in practice.

3.2.1 The Q grading

The grading Q on $\mathcal{G}$ will be computed additively from a grading $Q^* : \mathcal{Z} \to \mathbb{Z}$. Consider some $x \in \mathcal{Z}$, where $x \in \alpha_i \cap bE_j$.

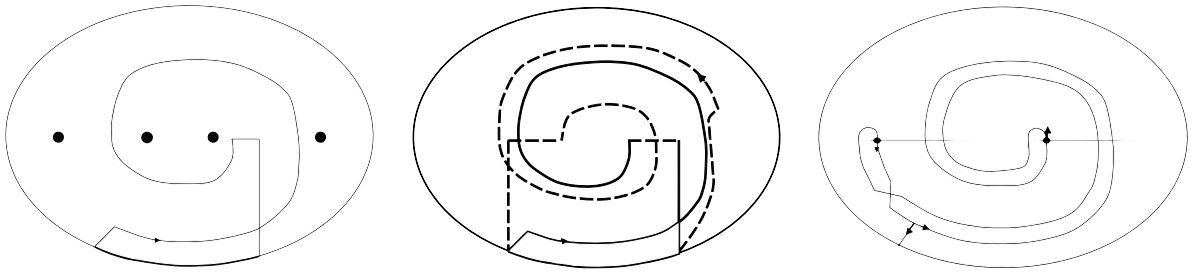

(a) A loop used for computing Q^*; the black dots are the punctures. Notice that $Q^*(x_3) = 2$.

(b) Two loops for computing T. Notice that $T(x_2x_3) = 3$.

(c) Tangent vectors used for computing P^*. Notice that $P^*(x_3) = 3$ and $P^*(x_1) = 0$.

Figure 9: Computing the gradings Q, T, and P

T	$\mathcal{G}$ elements
0	x_1x_4, x_1u, x_1u', tx_4, $t'x_4$
1	x_2v, x_2v', sx_3, $s'x_3$, sv, $s'v$, sv', $s'v'$
2	tu, $t'u$, tu', $t'u'$
3	x_2x_3

P^*	$\mathcal{Z}$ elements
0	x_1, x_4
1	s, v
2	s', t, u, v'
3	t', x_2, x_3, u'

P	$\mathcal{G}$ elements
0	x_1x_4
2	x_1u, tx_4, sv
3	x_1u', $t'x_4$, $s'v$, sv'
4	x_2v, sx_3, $s'v'$, tu
5	x_2v', $s'x_3$, $t'u$, tu'
6	x_2x_3, $t'u'$

Q^*	$\mathcal{Z}$ elements
0	x_1, v, x_4
1	v'
2	x_3, t, u, s
3	t', u', s'
4	x_2

Q	$\mathcal{G}$ elements
0	x_1x_4
2	x_1u, tx_4, sv
3	x_1u', $t'x_4$, $s'v$, sv'
4	x_2v, sx_3, $s'v'$, tu
5	x_2v', $s'x_3$, $t'u$, tu'
6	x_3x_3, $t'u'$

Table 1: Distributions of T, P^*, P, Q^*, and Q gradings for $\sigma_2^3 \in B_4$

Define an arc γ_x in the disk by starting at d_j, traveling along $-bh_j$ to bm_j, traveling along bE_j to x, traveling along α_i to m_i, and traveling along h_i to d_i. Then let γ_{ij} be the arc traveling along the lower portion of ∂D from d_i to d_j. Then $\gamma_x\gamma_{ij}$ is an arc from d_j to itself, and we define $Q^*(x)$ to be the winding number of this loop around the set of punctures.

Then for each $\mathbf{e} = e_1e_2 \dots e_n \in \mathcal{G}$, define

$$Q(\mathbf{e}) = \sum_{i=1}^{n} Q^*(e_i).$$

3.2.2 The T grading

Given $\mathbf{e} = e_1e_2 \dots e_n \in \mathcal{G}$, we have that for each k, $e_k = e_{x_k}$ or $e_k = e'_{x_k}$ for some $x_k \in \widetilde{\mathcal{Z}}$. Let $\mathbf{x} = x_1x_2 \dots x_n \in \widetilde{\mathcal{G}}$.

Then denote by $\tilde{\gamma}_{x_k}$ the arc obtained by replacing the figure-eight segments of γ_{x_k} with the

corresponding β arc segments. Then $T(\mathbf{x})$ can be computed as twice the sum of the pairwise winding of the $\tilde{\gamma}_{x_k}$ around each other. In other words, if $\tilde{\gamma}_{x_k}$ and $\tilde{\gamma}_{x_m}$ make a half-twist counter-clockwise around each other for $k \neq m$, this contributes $+1$ to the value of $T(\mathbf{x})$. Define $T : \mathcal{G} \to \mathbb{Z}$ by letting $T(\mathbf{e}) = T(\mathbf{x})$.

3.2.3 The P grading

This grading will be computed additively from a grading $P^* : \mathcal{Z} \to \mathbb{Z}$, which measures twice the relative winding number of the tangent vectors to the figure eights E'_k at the points in $\mathcal{Z}$.

For $x \in \mathcal{Z}$, where $x \in \alpha_i \cap bE_j$, we define $P^*(x)$ in the following way. We view the arc bh_j as being oriented downward at the point where it intersects ∂D. Let bE_j have the orientation induced by the orientation on E_j in the standard fork diagram. Then we let $P^*(x)$ be twice the winding number of the tangent vector relative to the downward-pointing tangent vector at the point $h'_j \cap \partial D$. In other words, if the tangent vector makes k counter-clockwise half-revolutions and m clockwise half-revolutions as we travel first along bh_j from $bh_j(0)$ to $bh_j(1)$ then along bE_j to x, then we set $P^*(x) = m - k$. This number is an integer because we assume that at any point $x \in \mathcal{Z}$, the figure-eight intersects the α arc at a right angle.

Then for $\mathbf{e} = e_1 e_2 \dots e_n \in \mathcal{G}$, we define

$$P(\mathbf{e}) = \sum_{i=1}^{n} P^*(e_i).$$

4 The anti-diagonal filtration

We review here how one obtains from the above picture a filtration on the Heegaard Floer complex, following Manolescu in [7] and Seidel and Smith in [18].

We'll first recall in Section 4.1 a formal construction involving graded totally-real submanifolds, as discussed by Manolescu in [7]. This repeats the construction of graded Lagrangians by Seidel in [16], following the ideas of Kontsevich in [5].

Then we'll apply the formalism in Section 4.1 to define Seidel gradings on two particular totally real tori in the n-fold symmetric product of a Riemann surface Σ. It is illustrated in [7] that by taking the Lagrangian Floer cohomology of these tori in the complement of a certain divisor $\bigtriangledown \subset Sym^n(\Sigma)$, one obtains the fixed-point symplectic Khovanov homology group $Kh_{symp,inv}(K)$. However, Manolescu also showed that these tori can be viewed as Heegaard tori $\mathbb{T}_{\widehat{\boldsymbol{\alpha}}}, \mathbb{T}_{\widehat{\boldsymbol{\beta}}}$ for the manifold $\Sigma(K)\#(S^2 \times S^1)$. A holomorphic volume form on $W = Sym^n(\Sigma) - \bigtriangledown$ induces an absolute Maslov grading $\widetilde{R}$ on intersections of these tori when viewed inside W.

Further, we have an identification of the set of Bigelow generators $\mathcal{G}$ with a generating set for the Heegaard Floer chain groups. This allows us to view $\widetilde{R}$ as a function on $\mathcal{G}$, and it in fact coincides with $P - Q + T$. However, when we view these tori inside all of $Sym^n(\Sigma)$, this grading is no longer a priori consistent with Maslov index calculations (but rather also records intersections of 2-gons with the factor $\bigtriangledown$).

We can use R (a shifted version of $\widetilde{R}$) to define a filtration ρ on $\widehat{CF}(\Sigma(K)\#(S^2 \times S^1), \mathfrak{s})$ for each torsion $\mathfrak{s} \in \mathrm{Spin}^c(\Sigma(K)\#(S^2 \times S^1))$. The definition for ρ will appear to depend heavily on the braid b chosen to represent the knot K. However, we'll obtain an invariance result for this filtration in Section 5.2 in the form of Theorem 1.

4.1 Graded totally real submanifolds

First recall the following definition:

Definition 17. A real subspace $V \subset \mathbb{C}^n$ is called **totally real** (with respect to the standard complex structure if $dim_{\mathbb{R}} V = n$ and $V \cap iV = 0$. A half-dimensonal submanifold $\mathcal{T}$ of an almost complex manifold (Y, J) is called **totally real** if $T_x\mathcal{T} \cap J(T_x\mathcal{T}) = 0$ for all $x \in \mathcal{T}$.

We'll first work in the setting of a Kähler manifold (Y, Ω) such that Ω is exact and $c_1(Y) = 0$. Furthermore, let $\mathcal{T}$ and $\mathcal{T}'$ be two totally real submanifolds of Y, intersecting transversely.

Under these conditions, there is a well-defined $\mathbb{Z}$-graded abelian group

$$HF^*(\mathcal{T}, \mathcal{T}') = H(CF^*(\mathcal{T}, \mathcal{T}'), d),$$

where the grading is relative (i.e. well-defined upto a constant shift), and is given by a Maslov index calculation. However, by a construction of Seidel in [16], this relative grading can be improved to an absolute $\mathbb{Z}$-grading.

Let $\mathfrak{T} \to Y$ be the natural fiber bundle whose fibers $\mathfrak{T}_x$ are the manifolds of totally real subspaces of T_xY. Choosing a complex volume form Θ on Y determines a square phase map $\theta : \mathfrak{T} \to \mathbb{C}^*/\mathbb{R}_+ \cong S^1$ given by

$$\theta(V) = \Theta(e_1 \wedge \ldots \wedge e_n)^2,$$

where $e_1, \ldots, e_n$ is any orthonormal basis for $V \subset T_xY$.

Let $\widetilde{\mathfrak{T}} \to \mathfrak{T}$ be the infinite cyclic covering obtained by pulling back the covering $\mathbb{R} \to S^1$ via the map θ. Consider the canonical section $s_{\mathcal{T}} : \mathcal{T} \to \mathfrak{T}$ given by $s_{\mathcal{T}}(x) = T_x\mathcal{T}$. This section induces a map

$$\theta_{\mathcal{T}} = \theta \circ s_{\mathcal{T}} : \mathcal{T} \to S^1.$$

In some cases, the section $s_{\mathcal{T}}$ can be lifted to a section $\widetilde{s}_{\mathcal{T}} : \mathcal{T} \to \widetilde{\mathfrak{T}}$ (inducing a lift $\widetilde{\theta}_{\mathcal{T}} : \mathcal{T} \to \mathbb{R}$ of the map $\theta_{\mathcal{T}}$). Let's assume such a lift exists.

Definition 18. A **grading** on $\mathcal{T}$ is a choice of lift $\widetilde{\theta}_{\mathcal{T}} : \mathcal{T} \to \mathbb{R}$.

Given such gradings on the submanifolds $\mathcal{T}$ and $\mathcal{T}'$, one can define the absolute Maslov index $\mu(x) \in \mathbb{Z}$ for each element $x \in \mathcal{T} \cap \mathcal{T}'$ [16]. This index is constructed using the Maslov index of paths in $\mathfrak{T}_x$, which is discussed in [13]. We'll sometimes refer to the grading structure on $\mathcal{T}$ as $\widetilde{\mathcal{T}}$, and we'll refer to the absolutely-graded Lagrangian Floer groups for the graded Lagrangians $\widetilde{\mathcal{T}}$ and $\widetilde{\mathcal{T}}'$ as $HF^*(\widetilde{\mathcal{T}}, \widetilde{\mathcal{T}}')$.

If $\Phi : Y \to Y$ is a symplectic automorphism, let $\Phi^{\mathfrak{T}} : \mathfrak{T} \to \mathfrak{T}$ denote the map given by $\Phi^{\mathfrak{T}}(V) = D\Phi(V)$. We recall the following definition:

Definition 19. Let $\Phi : Y \to Y$ be a symplectic automorphism, and suppose that there is a $\mathbb{Z}$-equivariant diffeomorphism $\widetilde{\Phi} : \widetilde{\mathfrak{T}} \mapsto \widetilde{\mathfrak{T}}$ which is a lift of $\Phi^{\mathfrak{T}}$. Then the pair $(\Phi, \widetilde{\Phi})$ is called a **graded symplectic automorphism**.

A graded symplectic automorphism $(\Phi, \widetilde{\Phi})$ acts on a graded Lagrangian submanifold $(L, \widetilde{L})$ by

$$(\Phi, \widetilde{\Phi})(L, \widetilde{L}) = (\Phi(L), \widetilde{\Phi} \circ \widetilde{L} \circ \Phi^{-1})$$

.

Remark 20. We'll often write $\widetilde{\Phi}$ to refer to the pair $(\Phi, \widetilde{\Phi})$ (and thus $\widetilde{\Phi}(\widetilde{L})$ will denote $(\Phi, \widetilde{\Phi})(L, \widetilde{L})$).

As discussed in [16], many Lagrangian Floer identities can be extended to the absolutely-graded case. For instance, as absolutely-graded complexes,

$$CF(\widetilde{\mathcal{T}}, \widetilde{\mathcal{T}}') \cong \left(CF(\widetilde{\mathcal{T}}, \widetilde{\mathcal{T}}')\right)^{\vee} \quad \text{(where } C^{\vee} \text{ denotes the dual complex of } C\text{)}.$$

Further, if $\widetilde{\Phi}$ is a graded symplectic automorphism, then there is a natural isomorphism of absolutely-graded complexes

$$CF(\widetilde{\Phi}(\widetilde{\mathcal{T}}), \widetilde{\Phi}(\widetilde{\mathcal{T}}')) \cong CF(\widetilde{\mathcal{T}}, \widetilde{\mathcal{T}}').$$

4.2 From fork diagrams to Heegaard Floer homology

We summarize Manolescu's work in [7], describing a connection between Bigelow's fork diagram and a Heegaard diagram for the manifold $\Sigma(K)\#(S^2 \times S^1)$.

We represent a knot K as the plat closure of a braid $b \in B_{2n}$, the braid group on $2n$ strands, and obtain a fork diagram for b by following the action the braid on the standard fork diagram, as described in Section 3.1.

Now let $P_\mu \in \mathbb{C}[t]$ be a polynomial with set of roots $\{\mu_1, \dots \mu_{2n}\}$, which is exactly the set of punctures in $\mathbb{C}$. We define an affine space $\widehat{S}$ by

$$\widehat{S} = \{(u, z) \in \mathbb{C}^2 : u^2 + P_\mu(z) = 0\} \subset \mathbb{C}^2.$$

Also , for $k = 1, \dots, n$, define the subspaces $\widehat{\alpha}_k$ and $\widehat{\beta}_k$ of $\widehat{S}$ by

$$\widehat{\alpha}_k = \{(u, z) \in \mathbb{C} : z = \alpha_k(t), \text{ for some } t \in [0, 1]; u = \pm\sqrt{-P_\mu(z)}\} \text{ and}$$
$$\widehat{\beta}_k = \{(u, z) \in \mathbb{C} : z = \beta_k(t), \text{ for some } t \in [0, 1]; u = \pm\sqrt{-P_\mu(z)}\}.$$

Notice that the map $\widehat{S} \to \mathbb{C}$ defined by $(u, z) \mapsto z$ is a double branched covering with branch set equal to $\{\mu_1, \dots, \mu_{2n}\} \subset \mathbb{C}$. This means that $\widehat{S}$ can be seen as $\Sigma_{n-1} - \{\pm\infty\}$, where Σ_{n-1} is a Riemann surface of genus $(n-1)$. Furthermore, the $\widehat{\alpha}_k$ and $\widehat{\beta}_k$ are simple closes curves in $\widehat{S}$ which induce totally real tori $\mathbb{T}_{\widehat{\boldsymbol{\alpha}}} = \widehat{\alpha}_1 \times \ldots \times \widehat{\alpha}_n, \mathbb{T}_{\widehat{\boldsymbol{\beta}}} = \widehat{\beta}_1 \times \ldots \times \widehat{\beta}_n \subset \mathrm{Sym}^n\left(\widehat{S}\right)$. We want a Heegaard diagram, so we stabilize this surface as shown in Figure 10 to acquire $\Sigma_n - \{\pm\infty\}$.

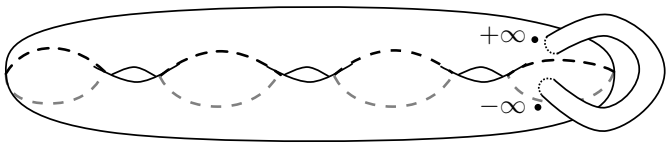

Figure 10: Stabilizing the surface Σ_{n-1} to obtain a Heegaard diagram

Proposition 21 (Proposition 7.4 from [7])**.** *The collection of data*

$$\mathcal{H} = (\Sigma_n; \widehat{\alpha}_1, \dots, \widehat{\alpha}_n; \widehat{\beta}_1, \dots, \widehat{\beta}_n; +\infty)$$

is an admissible pointed Heegaard diagram for $\Sigma(K)\#(S^2 \times S^1)$.

Now notice that with respect to the covering map above, each puncture $\mu_k \in \mathbb{C}$ has a single point as its preimage. However, the preimage of a point $x \in \beta_j \cap \text{int}(\alpha_i)$ consists of a pair of points upstairs. This gives a bijection between the intersection $\mathbb{T}_{\widehat{\boldsymbol{\alpha}}} \cap \mathbb{T}_{\widehat{\boldsymbol{\beta}}}$ and the set $\mathcal{G}$ of Bigelow generators as defined in Section 3.1. However, this identification isn't canonical, since for some $x \in \widetilde{\mathcal{Z}} - \tau$ it is only required that the pair $\{e_x, e'_x\}$ is identified with the two preimages of x upstairs.

4.3 A grading induced by a volume form

Define a subset $W = Sym^n(\widehat{S}) - \bigtriangledown$, where the anti-diagonal $\bigtriangledown$ is defined by

$$\bigtriangledown = \{(u_k, z_k), k = 1, \ldots, n : u_k^2 + P_\mu(z_k) = 0, (u_i, z_i) = (-u_j, z_j) \text{ for some } i \neq j\}$$

When we restrict to W, the Maslov grading on $\mathbb{T}_{\widehat{\boldsymbol{\alpha}}} \cap \mathbb{T}_{\widehat{\boldsymbol{\beta}}}$ can be lifted to an absolute Maslov $\mathbb{Z}$-grading by endowing the tori $\mathbb{T}_{\widehat{\boldsymbol{\alpha}}}$, $\mathbb{T}_{\widehat{\boldsymbol{\beta}}}$ with gradings in the sense of Section 4.1 via the choice of a particular holomorphic volume form.

Proposition 22 (Proposition 7.5 from [7])**.** *There exists a complex volume form Θ on W so that we can endow $\mathbb{T}_{\widehat{\boldsymbol{\alpha}}}$ and $\mathbb{T}_{\widehat{\boldsymbol{\beta}}}$ with gradings on the sense of Section 4.1. The resulting absolute Maslov grading (in W) on the elements of $\mathbb{T}_{\widehat{\boldsymbol{\alpha}}} \cap \mathbb{T}_{\widehat{\boldsymbol{\beta}}}$ is $P - Q + T$.*

Proof. We can apply most of Manolescu's braid closure proof to the plat closure case, establishing that $P - Q + T$ and the Maslov grading agree as relative gradings.

One obtains an absolute grading by requiring that the grading on $\mathbb{T}_{\widehat{\boldsymbol{\beta}}}$ to be obtained from the one on $\mathbb{T}_{\widehat{\boldsymbol{\alpha}}}$ by following the action on the punctured plane by the braid b in the following way. If $\mathbf{x}$ is the n-tuple whose components are the midpoints of the α_i and $\mathbf{y}$ is its image under the map induced by the braid b, then we require that $\widetilde{\theta}_{\widehat{\alpha}}(\mathbf{x})$ and $\widetilde{\theta}_{\widehat{\beta}}(\mathbf{y})$ lie on the same sheet of the cover $\mathbb{R} \to S^1$. This convention accounts for the handles utilized in our definitions for P, Q, and T in Section 3.2 , and so we obtain $P - Q + T$ on the nose.

□

We can now view $\widetilde{R}$ as a function both on $\mathbb{T}_{\widehat{\boldsymbol{\alpha}}} \cap \mathbb{T}_{\widehat{\boldsymbol{\beta}}}$ and on the set $\mathcal{G}$ of Bigelow generators. Now we define a rational number $s_R(b, D)$, which will depends on properties of the braid b and of the oriented link diagram D which is its plat closure. Denote by $\epsilon(b)$ the sum of the powers (with sign) of the braid group generators making up the word b, and denote by w the writhe of the diagram D. Then let

$$s_R(b, D) = \frac{\epsilon(b) - w(D) - 2n}{4} \in \mathbb{Q}.$$

Then for $\mathbf{e} \in \mathcal{G}$, define

$$R(\mathbf{e}) = \widetilde{R}(\mathbf{e}) + s_R = P(\mathbf{e}) - Q(\mathbf{e}) + T(\mathbf{e}) + s_R.$$

4.4 Computing R for the left-handed trefoil

Here we have that $n = 2$, $\epsilon = 3$, and $w = -3$, and so

$$s_R(b, D) = \frac{(3) - (-3) - 2(2)}{4} = \frac{1}{2}.$$

Combining this with Table 1, one obtains the distributions of $\widetilde{R}$ and R seen in Table 2.

$\widetilde{R}$	$\mathcal{G}$ elements
0	x_1x_4, x_1u, x_1u', tx_4, $t'x_4$
1	x_2v, x_2v', sx_3, $s'x_3$, sv, $s'v$, sv', $s'v'$
2	tu, $t'u$, tu', $t'u'$
3	x_2x_3

R	$\mathcal{G}$ elements
1/2	x_1x_4, x_1u, x_1u', tx_4, $t'x_4$
3/2	x_2v, x_2v', sx_3, $s'x_3$, sv, $s'v$, sv', $s'v'$
5/2	tu, $t'u$, tu', $t'u'$
7/2	x_2x_3

Table 2: Distributions of the gradings $\widetilde{R}$ and R for $\sigma_2^3 \in B_4$

One should notice that for any $x \in \widetilde{\mathcal{Z}} - \tau$, we have that $Q^*(e'_x) = Q^*(e_x) + 1$ and $P^*(e'_x) = P^*(e_x) + 1$. As a result, $R(e'_x\mathbf{y}) = R(e_x\mathbf{y})$; in the terminology from [7], the grading R is thus **stable**.

4.5 Intersections with the anti-diagonal

However, as observed in [18], the volume form Θ has an order-one zero along the antidiagonal $\bigtriangledown$. Therefore, R isn't compatible with Maslov index counts in all of $Sym^n(\widehat{S})$.

Let $\phi \in \pi_2(\mathbf{x}, \mathbf{y})$ be counted by a term in $\widehat{\partial}(\mathbf{x})$. If ϕ intersects $\bigtriangledown$ with multiplicity $k \in \mathbb{Z}$ (it can be arranged that $k \geq 0$, with equality only if ϕ completely avoids $\bigtriangledown$), then [18] gives that

$$R(\mathbf{x}) - R(\mathbf{y}) = 2k + 1.$$

More generally, one can say that if $\phi \in \pi_2(\mathbf{x}, \mathbf{y})$ with $n_{+\infty}(\phi) = 0$, then

$$R(\mathbf{x}) - R(\mathbf{y}) = \mu(\phi) + 2\left([\phi] \cdot [\bigtriangledown]\right) = gr(\mathbf{x}, \mathbf{y}) + 2\left([\phi] \cdot [\bigtriangledown]\right).$$

Now for each torsion $\mathfrak{s} \in \mathrm{Spin}^c(\Sigma(K)\#(S^2 \times S^1))$ define $\rho : \mathfrak{U}_\mathfrak{s} \to \mathbb{Q}$ by

$$\rho(\mathbf{x}) = R(\mathbf{x}) - \widetilde{gr}(\mathbf{x}).$$

Then we have that if $\mathbf{x}, \mathbf{y} \in \mathfrak{U}_\mathfrak{s}$ for $\mathfrak{s}$ torsion and $\phi \in \pi_2(\mathbf{x}, \mathbf{y})$ with $n_{+\infty}(\phi) = 0$,

$$\rho(\mathbf{x}) - \rho(\mathbf{y}) = 2[\phi] \cdot [\bigtriangledown].$$

Now ρ provides a filtration grading on the factor $\widehat{CF}(\mathcal{H}, \mathfrak{s})$ for each torsion $\mathfrak{s}$.

4.5.1 A schematic example of non-trivial intersection

For the sake of concreteness, let's see an example of a 2-gon whose intersection number with the anti-diagonal is nonzero. Figure 11 shows a portion of a fork diagram induced by some braid in B_6. Let $\mathbf{x}, \mathbf{y} \in \mathcal{G}$ be the Bigelow generators whose components are indicated in Figure 11.

Figure 12 shows the Heegaard diagram of genus 3 obtained from the fork diagram via Theorem 21, and let π denote the branched covering map. Let $\widehat{\mathbf{x}}, \widehat{\mathbf{y}} \in \mathbb{T}_{\widehat{\boldsymbol{\alpha}}} \cap \mathbb{T}_{\widehat{\boldsymbol{\beta}}}$ have components as indicated in the Heegaard diagram, where $\pi(\widehat{x}_i) = x_i$ and $\pi(\widehat{y}_i) = y_i$ for $i = 1, 2, 3$. The shaded region in Figure 12 is the domain $\mathcal{D}(\phi)$ of a 2-gon $\phi \in \pi_2(\widehat{\mathbf{x}}, \widehat{\mathbf{y}})$ and the shaded region in Figure 11 is its image $\pi(\mathcal{D}\phi)$.

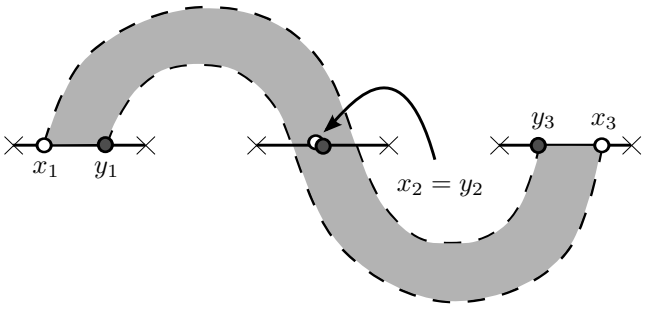

Figure 11: A portion of a fork diagram. The domain $\pi(\mathcal{D}(\phi))$ is shaded, the $\boldsymbol{\alpha}$ arcs are solid, and the $\boldsymbol{\beta}$ arcs are dashed.

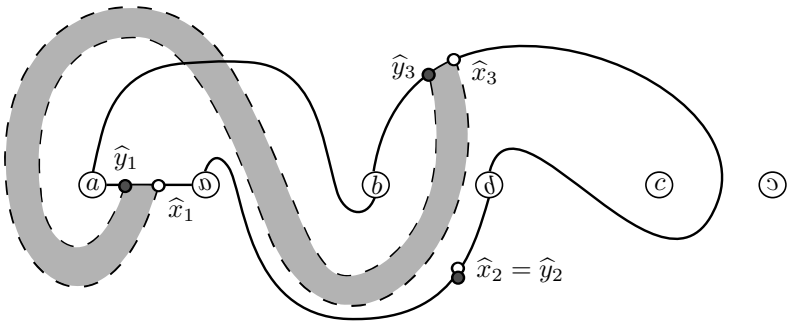

Figure 12: A Heegaard diagram induced by Figure 11. The domain $\mathcal{D}(\phi)$ is shaded.

Notice that for each i, $\pi^{-1}(x_i)$ contains two points; the point $\widehat{x}_2$ and $\widehat{y}_2$ are both chosen to be the preimage of $x_2 = y_2$ which lies outside of the domain $\mathcal{D}(\phi)$.

One can see that $\widehat{gr}(\widehat{\mathbf{x}}) - \widehat{gr}(\widehat{\mathbf{y}}) = \mu(\phi) = 1$. However, $[\phi] \cdot [\bigtriangledown] = 1$, and one can verify from the fork diagram that indeed $R(\mathbf{x}) - R(\mathbf{y}) = 3$.

4.5.2 The anti-diagonal and Heegaard multi-diagrams

We'll find in Section 5 that Birman moves will induce sequences of Heegaard moves such that only the initial and final α and β circles are lifts of arcs from fork diagrams. However, one should consider $\bigtriangledown \subset Sym^n(\Sigma)$ as being determined by the branched covering map $\Sigma \to \mathbb{C}$ (and thus being a well-defined feature of intermediate Heegaard diagrams).

Notice that because the local pictures of Σ which we study are exactly the branched double-covers of our local fork diagrams, we needn't worry about regions in the local domains intersecting branched covering "twins" of points outside of the local areas. Also, regions of these domains which lie outside of the local pictures will be "thin" regions. Thus to investigate intersections of our 3-gons with $\bigtriangledown$, it suffices to study regions in the domains of these 3-gons which lie within our local pictures of Σ. Furthermore, non-trivial intersection with $\bigtriangledown$ can only potentially occur when two or more components of affected generators lie within the local picture).

5 Invariance of the filtration

Here we'll prove a few facts that we'll use in our invariance proofs.

Remark 23. From now on, we'll suppress the hat when discussing a lift $\widehat{\alpha}$ of an arc α unless the distinction isn't obvious from the context.

Now let $(\Sigma;\boldsymbol{\alpha}';\boldsymbol{\alpha};\boldsymbol{\beta};z)$ be an admissible pointed Heegaard triple-diagram of genus n, where the set of attaching circles $\boldsymbol{\alpha}'$ is obtained from $\boldsymbol{\alpha}$ via a handleslide or an isotopy. Assume that for each k, α_k' has been chosen such that it intersects α_k transversely in exactly two points. Then $(\Sigma;\boldsymbol{\alpha};\boldsymbol{\beta};z)$ and $(\Sigma;\boldsymbol{\alpha}';\boldsymbol{\beta};z)$ are two admissible pointed Heegaard diagrams for a the same 3-manifold M. Recall that in fact $(\Sigma;\boldsymbol{\alpha}';\boldsymbol{\alpha};z)$ is an admissible pointed Heegaard diagram for $\#_n(S^1\times S^2)$. There is a natural choice of top-degree generator $\boldsymbol{\theta}_{\boldsymbol{\alpha}'\boldsymbol{\alpha}}\in\mathbb{T}_{\boldsymbol{\alpha}'}\cap\mathbb{T}_{\boldsymbol{\alpha}}$.

Further, for any $\mathbf{x}\in\mathbb{T}_{\boldsymbol{\alpha}'}\cap\mathbb{T}_{\boldsymbol{\alpha}}$, $\mathbf{y}\in\mathbb{T}_{\boldsymbol{\alpha}}\cap\mathbb{T}_{\boldsymbol{\beta}}$, and $\mathbf{x}\in\mathbb{T}_{\boldsymbol{\alpha}'}\cap\mathbb{T}_{\boldsymbol{\beta}}$, there is a well-defined map

$$\mathfrak{s}_z:\pi_2(\mathbf{x},\mathbf{y},\mathbf{x})\to \mathrm{Spin}^c(X),$$

where X is the cobordism induced by the move. Since X is induced by a handleslide or any isotopy, it is in fact the identity cobordism. Therefore, if $\boldsymbol{\theta}_{\boldsymbol{\alpha}'\boldsymbol{\alpha}}\in\mathbb{T}_{\boldsymbol{\alpha}'}\cap\mathbb{T}_{\boldsymbol{\alpha}}$ represents the top-degree generator of $\widehat{CF}(\#^n(S^2\times S^1))$, then for some $\psi\in\pi_2(\boldsymbol{\theta}_{\boldsymbol{\alpha}'\boldsymbol{\alpha}},\mathbf{y},\mathbf{z})$, $\mathfrak{s}_z(\psi)$ is completely determined by either restriction $\mathfrak{s}_z(\mathbf{y})$ or $\mathfrak{s}_z(\mathbf{z})$.

Letting $\widetilde{\boldsymbol{\alpha}}$ be obtained from $\boldsymbol{\alpha}$ via small isotopic translates and working in the pointed Heegaard quadruple-diagram $(\Sigma;\widetilde{\boldsymbol{\alpha}};\boldsymbol{\alpha}';\boldsymbol{\alpha};\boldsymbol{\beta};z)$, one can make an analogous observation regarding Spin^c structures associated to 4-gons.

Recall that the filtration ρ is only well-defined on the factors

$$\widehat{CF}(\Sigma(K)\#(S^2\times S^1),\mathfrak{s}) \text{ with } \mathfrak{s}\in\mathrm{Spin}^c(\Sigma(K)\#(S^2\times S^1)) \text{ torsion.}$$

However, due to the observations above, everything in sight will be Spin^c-equivalent and we will supress Spin^c structures in notation when proving the lemmas in this section.

Below we discuss Heegaard diagrams obtained from braids. The Birman stabilization move on braids induces in the Heegaard diagram a Heegaard stabilization followed by two handleslides. For a Heegaard diagram $\mathcal{H}$, stabilization amounts to taking a connected sum with $\mathcal{H}_0$, the standard genus-one diagram for S^3 with $\boldsymbol{\alpha}\cap\boldsymbol{\beta}=\{x\}$. Ozsváth and Szabó showed in [10] that as chain complexes, $\widehat{CF}(\mathcal{H})\cong\widehat{CF}(\mathcal{H}\#\mathcal{H}_0)$. If $\mathcal{H}$ is a Heegaard diagram for $\Sigma(K)\#(S^2\times S^1)$ obtained from a braid b, we extend R and ρ to $\widehat{CF}(\mathcal{H}\#\mathcal{H}_0,\mathfrak{s}\#\mathfrak{s}_0)$ for each torsion $\mathfrak{s}$ by setting $R(x\mathbf{y})=R(\mathbf{y})$.

Let's first establish some terminology that will be used in the lemmas to follow.

Definition 24. Let $(\Sigma;\boldsymbol{\alpha};\boldsymbol{\beta};z)$ and $\left(\Sigma;\boldsymbol{\alpha}';\boldsymbol{\beta}';z\right)$ be two Heegaard diagrams of genus n arising from braids b and b' (possibly after Heegaard stabilization) and suppose that $\boldsymbol{\alpha}'$ (respectively $\boldsymbol{\beta}'$) is obtained from $\boldsymbol{\alpha}$ (respectively $\boldsymbol{\beta}$) via a sequence of handleslides and isotopies.

(i) An **$\boldsymbol{\alpha}$-triangle injection** is a function $g:\mathbb{T}_{\boldsymbol{\alpha}}\cap\mathbb{T}_{\boldsymbol{\beta}}\hookrightarrow\mathbb{T}_{\boldsymbol{\alpha}'}\cap\mathbb{T}_{\boldsymbol{\beta}}$ such that the following hold:

  (a) There is a Heegaard triple-diagram $(\Sigma;\boldsymbol{\alpha}^+;\boldsymbol{\alpha};\boldsymbol{\beta};z)$ (where for each k, α_k^+ is isotopic to α_k' and intersects α_k transversely in two points) such that for each $\mathbf{x}\in\mathbb{T}_{\boldsymbol{\alpha}}\cap\mathbb{T}_{\boldsymbol{\beta}}$, there is a 3-gon class $\psi_g^+\in\pi_2(\boldsymbol{\theta}_{\boldsymbol{\alpha}^+\boldsymbol{\alpha}},\mathbf{x},\mathbf{y}^+)$ with $\mu(\psi_g^+)=0$, $\psi_g^+\cap\bigtriangledown=\emptyset$, and $n_z(\psi_g^+)=0$, where $\mathbf{y}^+\in\mathbb{T}_{\boldsymbol{\alpha}}\cap\mathbb{T}_{\boldsymbol{\alpha}^+}$ is nearest neighbor to $g(\mathbf{x})$.

  (b) There is a Heegaard triple-diagram $(\Sigma;\boldsymbol{\alpha};\boldsymbol{\alpha}^-;\boldsymbol{\beta};z)$ (where for each k, α_k^- is isotopic to α_k' and intersects α_k transversely in two points) such that for each $\mathbf{x}\in\mathbb{T}'_{\boldsymbol{\alpha}}\cap\mathbb{T}_{\boldsymbol{\beta}}$, there is a 3-gon class $\psi_g^-\in\pi_2(\boldsymbol{\theta}_{\boldsymbol{\alpha}\boldsymbol{\alpha}^-},\mathbf{y}^-,\mathbf{x})$ with $\mu(\psi_g^-)=0$, $\psi_g^-\cap\bigtriangledown=\emptyset$, and $n_z(\psi_g^-)=0$, where $\mathbf{y}^-\in\mathbb{T}_{\boldsymbol{\alpha}}\cap\mathbb{T}_{\boldsymbol{\alpha}^-}$ is nearest neighbor to $g(\mathbf{x})$.

(ii) A **$\boldsymbol{\beta}$-triangle injection** is a function $g:\mathbb{T}_{\boldsymbol{\alpha}}\cap\mathbb{T}_{\boldsymbol{\beta}}\hookrightarrow\mathbb{T}_{\boldsymbol{\alpha}}\cap\mathbb{T}_{\boldsymbol{\beta}'}$ such that the following hold:

(a) There is a Heegaard triple-diagram $\left(\Sigma;\boldsymbol{\alpha};\boldsymbol{\beta};\boldsymbol{\beta}^+;z\right)$ (where for each k, β_k^+ is isotopic to β_k' and intersects β_k transversely in two points) such that for each $\mathbf{x}\in\mathbb{T}_{\boldsymbol{\alpha}}\cap\mathbb{T}_{\boldsymbol{\beta}}$, there is a 3-gon class $\psi_g^+\in\pi_2(\mathbf{x},\boldsymbol{\theta}_{\boldsymbol{\beta}\boldsymbol{\beta}^+},\mathbf{y}^+)$ with $\mu(\psi_g^+)=0$, $\psi_g^+\cap\bigtriangledown=\emptyset$, and $n_z(\psi_g^+)=0$, where $\mathbf{y}^+\in\mathbb{T}_{\boldsymbol{\beta}}\cap\mathbb{T}_{\boldsymbol{\beta}^+}$ is nearest neighbor to $g(\mathbf{x})$.

(b) There is a Heegaard triple-diagram $\left(\Sigma;\boldsymbol{\alpha};\boldsymbol{\beta}^-;\boldsymbol{\beta};z\right)$ (where for each k, β_k^- is isotopic to β_k' and intersects β_k transversely in two points) such that for each $\mathbf{x}\in\mathbb{T}_{\boldsymbol{\alpha}}\cap\mathbb{T}'_{\boldsymbol{\beta}}$, there is a 3-gon class $\psi_g^-\in\pi_2(\mathbf{y}^-,\boldsymbol{\theta}_{\boldsymbol{\beta}^-\boldsymbol{\beta}},\mathbf{x})$ with $\mu(\psi_g^-)=0$, $\psi_g^-\cap\bigtriangledown=\emptyset$, and $n_z(\psi_g^-)=0$, where $\mathbf{y}^-\in\mathbb{T}_{\boldsymbol{\beta}}\cap\mathbb{T}_{\boldsymbol{\beta}^-}$ is nearest neighbor to $g(\mathbf{x})$.

Remark 25. From now on, we'll make no notational distinction between nearest neighbor points when discussing triangle injections; this distinction will be explicit when we discuss 4-gon-counting maps. Furthermore, the reader should note that everything in sight avoids the basepoint z.

We can then prove a fact about α-triangle injections regarding the R-filtration; there is an analogous version for β-triangle injections.

Lemma 26. *Let $\mathcal{H}_{\boldsymbol{\alpha}\boldsymbol{\beta}}=(\Sigma;\boldsymbol{\alpha};\boldsymbol{\beta};z)$ and $\mathcal{H}_{\boldsymbol{\alpha}'\boldsymbol{\beta}}=(\Sigma;\boldsymbol{\alpha}';\boldsymbol{\beta};z)$ be two pointed Heegaard diagrams for the manifold $\Sigma(K)\#(S^2\times S^1)$ which are obtained from braids b and b' (possibly after Heegaard stabilization), where*

$$\boldsymbol{\alpha}=\boldsymbol{\alpha}^0\to\boldsymbol{\alpha}^1\to\ldots\to\boldsymbol{\alpha}^n=\boldsymbol{\alpha}'$$

is a sequence of handleslides or isotopies. Also, let $g=g^n\circ\ldots\circ g^1$ be a composition of α-triangle injections

$$g^k:\mathbb{T}_{\boldsymbol{\alpha}^{k-1}}\cap\mathbb{T}_{\boldsymbol{\beta}}\to\mathbb{T}_{\boldsymbol{\alpha}^k}\cap\mathbb{T}_{\boldsymbol{\beta}}.$$

Let $f^k:\widehat{CF}(\mathcal{H}_{\boldsymbol{\alpha}^{k-1}\boldsymbol{\beta}})\to\widehat{CF}(\mathcal{H}_{\boldsymbol{\alpha}^k\boldsymbol{\beta}})$ be the chain homotopy equivalence induces by the k^{th} move and let $h^k:\widehat{CF}(\mathcal{H}_{\boldsymbol{\alpha}^k\boldsymbol{\beta}})\to\widehat{CF}(\mathcal{H}_{\boldsymbol{\alpha}^{k-1}\boldsymbol{\beta}})$ be its homotopy inverse. For the maps $f=f^n\circ\ldots\circ f^1$ and $h=h^1\circ\ldots\circ h^n$, let $H:\widehat{CF}(\mathcal{H}_{\boldsymbol{\alpha}\boldsymbol{\beta}})\to\widehat{CF}(\mathcal{H}_{\boldsymbol{\alpha}\boldsymbol{\beta}})$ and $G:\widehat{CF}(\mathcal{H}_{\boldsymbol{\alpha}'\boldsymbol{\beta}})\to\widehat{CF}(\mathcal{H}_{\boldsymbol{\alpha}'\boldsymbol{\beta}})$ be the natural 4-gon-counting homotopies such that

$$hf-id_{\widehat{CF}(\mathcal{H}_{\boldsymbol{\alpha}\boldsymbol{\beta}})}=\widehat{\partial}H+H\widehat{\partial}\quad\textit{and}\quad fh-id_{\widehat{CF}(\mathcal{H}_{\boldsymbol{\alpha}'\boldsymbol{\beta}})}=\widehat{\partial}G+G\widehat{\partial}.$$

Then for each torsion $\mathfrak{s}\in Spin^c(\Sigma(K)\#(S^2\times S^1))$, the following hold:

(i) If $\mathbf{y}\in\mathbb{T}_{\boldsymbol{\alpha}'}\cap\mathbb{T}_{\boldsymbol{\beta}}$ is a term in the sum $f(\mathbf{x})$ for some $\mathbf{x}\in\mathfrak{U}_{\mathfrak{s}}\subset\mathbb{T}_{\boldsymbol{\alpha}}\cap\mathbb{T}_{\boldsymbol{\beta}}$ and if $\mathbf{w}\in\mathbb{T}_{\boldsymbol{\alpha}}\cap\mathbb{T}_{\boldsymbol{\beta}}$ is a term in the sum $h(\mathbf{z})$ for some $\mathbf{z}\in\mathfrak{U}'_{\mathfrak{s}}\subset\mathbb{T}_{\boldsymbol{\alpha}'}\cap\mathbb{T}_{\boldsymbol{\beta}}$, then

$$R(\mathbf{y})\leq R(g(\mathbf{x}))\quad\textit{and}\quad R(\mathbf{z})\geq R(g(\mathbf{w})).$$

(ii) If $\mathbf{y}\in\mathbb{T}_{\boldsymbol{\alpha}}\cap\mathbb{T}_{\boldsymbol{\beta}}$ is a term in the sum $H(\mathbf{x})$ for some $\mathbf{x}\in\mathfrak{U}_{\mathfrak{s}}\subset\mathbb{T}_{\boldsymbol{\alpha}}\cap\mathbb{T}_{\boldsymbol{\beta}}$ and if $\mathbf{w}\in\mathbb{T}_{\boldsymbol{\alpha}'}\cap\mathbb{T}_{\boldsymbol{\beta}}$ is a term in the sum $G(\mathbf{z})$ for some $\mathbf{z}\in\mathfrak{U}'_{\mathfrak{s}}\subset\mathbb{T}_{\boldsymbol{\alpha}'}\cap\mathbb{T}_{\boldsymbol{\beta}}$, then

$$\rho(\mathbf{y})\leq\rho(\mathbf{x})\quad\textit{and}\quad\rho(\mathbf{w})\leq\rho(\mathbf{z}).$$

Proof of part (i). We work in the pointed Heegaard triple-diagrams of the form

$$\left(\Sigma;\boldsymbol{\alpha}^k;\boldsymbol{\alpha}^{k-1};\boldsymbol{\beta};z\right).$$

Let $\mathbf{x} \in \mathfrak{U}_{\mathfrak{s}} \subset \mathbb{T}_{\boldsymbol{\alpha}} \cap \mathbb{T}_{\boldsymbol{\beta}}$ and let $\mathbf{y}^1 \in \mathbb{T}_{\boldsymbol{\alpha}^1} \cap \mathbb{T}_{\boldsymbol{\beta}}$ be a term in the sum $f^1(\mathbf{x})$. Then there is a 3-gon class $\psi_{f^1} \in \pi_2(\boldsymbol{\theta}_{\boldsymbol{\alpha}^1\boldsymbol{\alpha}}, \mathbf{x}, \mathbf{y}^1)$ with pseudo-holomorphic representative such that $\mu(\psi_{f^1}) = 0$. Also, there is a 3-gon class $\psi_{g^1} \in \pi_2(\boldsymbol{\theta}_{\boldsymbol{\alpha}^1\boldsymbol{\alpha}}, \mathbf{x}, g^1(\mathbf{x}))$ with $\mu(\psi_{g^1}) = 0$ and $\psi_{g^1} \cap \bigtriangledown = \emptyset$ provided by the triangle injection g^1. The classes ψ_{f^1} and ψ_{g^1} are Spin^c-equivalent, and thus there are 2-gons $\eta_{\boldsymbol{\alpha}\boldsymbol{\beta}} \in \pi_2(\mathbf{x}, \mathbf{x})$, $\eta_{\boldsymbol{\alpha}^1\boldsymbol{\beta}} \in \pi_2(g^1(\mathbf{x}), \mathbf{y}^1)$, and $\eta_{\boldsymbol{\alpha}^1\boldsymbol{\alpha}} \in \pi_2(\boldsymbol{\theta}_{\boldsymbol{\alpha}^1\boldsymbol{\alpha}}, \boldsymbol{\theta}_{\boldsymbol{\alpha}^1\boldsymbol{\alpha}})$ such that

$$\psi_{f^1} = \psi_{g^1} + \eta_{\boldsymbol{\alpha}\boldsymbol{\beta}} + \eta_{\boldsymbol{\alpha}^1\boldsymbol{\beta}} + \eta_{\boldsymbol{\alpha}^1\boldsymbol{\alpha}}.$$

Now $\mathcal{D}(\eta_{\boldsymbol{\alpha}\boldsymbol{\beta}}), \mathcal{D}(\eta_{\boldsymbol{\alpha}^1\boldsymbol{\alpha}}) \in \Pi_{\boldsymbol{\alpha}\boldsymbol{\beta}\boldsymbol{\alpha}^1}$ are triply-periodic, and by Proposition 9 can be written as a sum of the "thin" doubly-periodic domains $\mathcal{D}_k^{\boldsymbol{\alpha}\boldsymbol{\alpha}^1} \in \Pi_{\boldsymbol{\alpha}\boldsymbol{\alpha}^1}$. Let $\eta_k^1 \in \pi_2(\boldsymbol{\theta}_{\boldsymbol{\alpha}^1\boldsymbol{\alpha}}, \boldsymbol{\theta}_{\boldsymbol{\alpha}^1\boldsymbol{\alpha}})$ denote the 2-gon whose components are given by $\mathcal{D}_k^{\boldsymbol{\alpha}\boldsymbol{\alpha}^1}$ in one copy of Σ and constant $\boldsymbol{\theta}_{\boldsymbol{\alpha}^1\boldsymbol{\alpha}}$ in the remaining $g-1$ copies. It can be arranged that the 2-gons η_k^1 avoid the anti-diagonal $\bigtriangledown \subset Sym^g(\Sigma)$ and the basepoint z. The class $\eta = \eta_{\boldsymbol{\alpha}\boldsymbol{\beta}} + \eta_{\boldsymbol{\alpha}^1\boldsymbol{\alpha}}$ can be written as a sum of elements of classes in $\{\eta_1^1, \ldots, \eta_g^1\}$, and thus $[\eta] \cdot [\bigtriangledown] = n_z(\eta) = 0$. Thus,

$$\mu(\eta_{\boldsymbol{\alpha}^1\boldsymbol{\beta}}) = \mu(\psi_{f^1}) - \mu(\psi_{g^1}) - \mu(\eta) = 0 - 0 - 0 = 0 \quad \text{and}$$
$$[\eta_{\boldsymbol{\alpha}^1\boldsymbol{\beta}}] \cdot [\bigtriangledown] = [\psi_{f^1}] \cdot [\bigtriangledown] - [\psi_{g^1}] \cdot [\bigtriangledown] - [\eta] \cdot [\bigtriangledown] = [\psi_{f^1}] \cdot [\bigtriangledown] - 0 - 0 \geq 0.$$

Then if $\mathbf{y}^2 \in \mathbb{T}_{\boldsymbol{\alpha}^2} \cap \mathbb{T}_{\boldsymbol{\beta}}$ is a term in $f^2(\mathbf{y}^1)$, let $\psi_{f^2} \in \pi_2(\boldsymbol{\theta}_{\boldsymbol{\alpha}^2\boldsymbol{\alpha}^1}, \mathbf{y}^1, \mathbf{y}^2)$ be a class with pseudo-holomorphic representative such that $\mu(\psi_{f^2}) = 0$. Then the concatenation $(\psi_{f^2} + \eta)$ is an element of $\pi_2(\boldsymbol{\theta}_{\boldsymbol{\alpha}^2\boldsymbol{\alpha}^1}, g^1(\mathbf{x}), \mathbf{y}^2)$. The triangle injection g^2 guarantees a 3-gon class $\psi_{g^2} \in \pi_2(\boldsymbol{\theta}_{\boldsymbol{\alpha}^2\boldsymbol{\alpha}^1}, g^1(\mathbf{x}), ((g^2 \circ g^1)(\mathbf{x}))$ such that $\mu(\psi_{g^2}) = 0$ and $\psi_{g^2} \cap \bigtriangledown = \emptyset$. Continuing this process, for each $\mathbf{y} \in \mathbb{T}_{\boldsymbol{\alpha}'} \cap \mathbb{T}_{\boldsymbol{\beta}}$ appearing as a term in the sum $(f^n \circ \ldots \circ f^1)(\mathbf{x})$, one can obtain a 2-gon $\phi \in \pi_2(g(\mathbf{x}), \mathbf{y})$ with

$$\mu(\phi) = 0 \quad \text{and} \quad [\phi] \cdot [\bigtriangledown] \geq 0.$$

On the other hand, let $\mathbf{z} \in \mathfrak{U}'_{\mathfrak{s}} \subset \mathbb{T}_{\boldsymbol{\alpha}'} \cap \mathbb{T}_{\boldsymbol{\beta}}$ and let $\mathbf{w}^{n-1}$ be a term in the sum $h^n(\mathbf{z})$. Let $\mathbf{u}^n = g^n(\mathbf{w}^{n-1})$. Then there is a (pseudo-holomorphic) class $\psi_{h^n} \in \pi_2(\boldsymbol{\theta}_{\boldsymbol{\alpha}^{n-1}\boldsymbol{\alpha}^n}, \mathbf{z}, \mathbf{w}^{n-1})$ and a (not necessarily pseudo-holomorphic) class $\psi'_{g^n} \in \pi_2(\boldsymbol{\theta}_{\boldsymbol{\alpha}^{n-1}\boldsymbol{\alpha}^n}, \mathbf{u}^n, \mathbf{w}^{n-1})$. One can see that continuing this process in a manner that is similar to the one for the f^i maps will produce, for each $\mathbf{w}$ appearing in the sum $h(\mathbf{z})$, a 2-gon $\phi' \in \pi_2(\mathbf{z}, g(\mathbf{w}))$ such that

$$\mu(\phi') = 0 \quad \text{and} \quad [\phi'] \cdot [\bigtriangledown] \geq 0.$$

□

Proof of part (ii). We work in the pointed Heegaard quadruple-diagrams of the form

$$\left(\Sigma; \widetilde{\boldsymbol{\alpha}}^{k-1}; \boldsymbol{\alpha}^k; \boldsymbol{\alpha}^{k-1}; \boldsymbol{\beta}; z\right),$$

where $\widetilde{\boldsymbol{\alpha}}^k$ is a set of attaching circles obtained from $\boldsymbol{\alpha}^k$ by small isotopies, with $\widetilde{\alpha}_i^k$ intersecting α_i^k transversely in two points.

We can write H in terms of homotopies $H^i : \widehat{CF}(Y_{\boldsymbol{\alpha}^i\boldsymbol{\beta}}) \to \widehat{CF}(Y_{\boldsymbol{\alpha}^i\boldsymbol{\beta}})$, which are 4-gon-counting maps as seen in Section 2.1.2. Indeed,

$$H = H^0 + h^1 \circ H^1 \circ f^1 + \ldots + \left(h^1 \circ \ldots \circ h^{n-1}\right) \circ H^{n-1} \circ \left(f^{n-1} \circ \ldots \circ f^1\right).$$

Suppose that $\mathbf{y} \in \mathbb{T}_{\boldsymbol{\alpha}} \cap \mathbb{T}_{\boldsymbol{\beta}}$ is a term in $\left(h^1 \circ \ldots \circ h^k\right) \circ H^k \circ \left(f^k \circ \ldots \circ f^1\right)(\mathbf{x})$. Again denote by $\mathbf{v} \mapsto \widetilde{\mathbf{v}}$ the associated nearest-neighbor map. Then there are $\mathbf{z}^j, \mathbf{u}^j \in \mathbb{T}_{\boldsymbol{\alpha}^j} \cap \mathbb{T}_{\boldsymbol{\beta}}$ for $j = 0, \ldots, k$

with $\mathbf{z}^0 = \mathbf{x}$, $\mathbf{u}^0 = \mathbf{y}$, $\mathbf{z}^i$ a term in $f^i(\mathbf{z}^{i-1})$, $\widetilde{\mathbf{u}}^k$ a term in $H^k(\mathbf{z}^k)$, and $\mathbf{u}^{i-1}$ a term in $h^i(\mathbf{u}^i)$ for $i = 1, \dots, k$.

We then have associated pseudo-holomorphic 3-gon classes $\psi_{f^i} \in \pi_2(\boldsymbol{\theta}_{\boldsymbol{\alpha}^i\boldsymbol{\alpha}^{i-1}}, \mathbf{z}^{i-1}, \mathbf{z}^i)$ and $\psi_{h^i} \in \pi_2(\boldsymbol{\theta}_{\boldsymbol{\alpha}^{i-1}\boldsymbol{\alpha}^i}, \mathbf{u}^i, \mathbf{u}^{i-1})$ for $i = 1, \dots, k$, as well as a pseudo-holomorphic 4-gon class $\rho \in \pi_2(\boldsymbol{\theta}_{\widetilde{\boldsymbol{\alpha}}^k\boldsymbol{\alpha}^{k+1}}, \boldsymbol{\theta}_{\boldsymbol{\alpha}^{k+1}\boldsymbol{\alpha}^k}, \mathbf{z}^k, \widetilde{\mathbf{u}}^k)$, such that

$$\mu(\psi_{f^i}) = \mu(\psi_{h^i}) = 0, \quad \mu(\rho) = -1, [\psi_{f^i}] \cdot [\bigtriangledown] \geq 0, \quad [\psi_{h^i}] \cdot [\bigtriangledown] \geq 0, \quad \text{and} \quad [\rho] \cdot [\bigtriangledown] \geq 0.$$

Now $\widetilde{gr}(\mathbf{z}^j) - \widetilde{gr}(\mathbf{u}^j) = \widetilde{gr}(\mathbf{z}^k) - \widetilde{gr}(\mathbf{u}^k) = \widetilde{gr}(\mathbf{z}^k) - \widetilde{gr}(\widetilde{\mathbf{u}^k}) = \mu(\rho) = -1$ and $\mathfrak{s}_z(\mathbf{u}^j) = \mathfrak{s}_z(\mathbf{z}^j)$ for each $j = 0, \dots, k$, and so there are 2-gon classes $\zeta^j \in \pi_2(\mathbf{z}^j, \mathbf{u}^j)$ such that $\mu(\zeta^j) = -1$. There are also index-zero 3-gon classes $\widetilde{\psi} \in \pi_2(\boldsymbol{\theta}_{\widetilde{\boldsymbol{\alpha}}^k\boldsymbol{\alpha}^k}, \mathbf{u}^k, \widetilde{\mathbf{u}}^k)$ and $\psi_\theta \in \pi_2(\boldsymbol{\theta}_{\widetilde{\boldsymbol{\alpha}}^k\boldsymbol{\alpha}^{k+1}}, \boldsymbol{\theta}_{\boldsymbol{\alpha}^{k+1}\boldsymbol{\alpha}^k}, \boldsymbol{\theta}_{\widetilde{\boldsymbol{\alpha}}^k\boldsymbol{\alpha}^k})$, and it can be arranged that $\widetilde{\psi} \cap \bigtriangledown = \psi_\theta \cap \bigtriangledown = \emptyset$.

Notice that $\widetilde{\psi} + \psi_\theta + \zeta^k \in \pi_2(\boldsymbol{\theta}_{\widetilde{\boldsymbol{\alpha}}^k\boldsymbol{\alpha}^{k+1}}, \boldsymbol{\theta}_{\boldsymbol{\alpha}^{k+1}\boldsymbol{\alpha}^k}, \mathbf{z}^k, \widetilde{\mathbf{u}}^k)$, and so there is some 4-gon η with quadruply-periodic domain such that

$$\widetilde{\psi} + \psi_\theta + \zeta^k = \rho + \eta.$$

But recall that η can be written as the concatenation of 2-gons which avoid the anti-diagonal $\bigtriangledown$ and the basepoint z, and so

$$[\zeta^k] \cdot [\bigtriangledown] = [\rho] \cdot [\bigtriangledown] + [\eta] \cdot [\bigtriangledown] - [\widetilde{\psi}] \cdot [\bigtriangledown] - [\psi_\theta] \cdot [\bigtriangledown] = [\rho] \cdot [\bigtriangledown] + 0 - 0 - 0 \geq 0.$$

Furthermore, the α-triangle injections guarantee points $\mathbf{w}^j \in \mathbb{T}_{\boldsymbol{\alpha}^j} \cap \mathbb{T}_{\boldsymbol{\beta}}$ for $j = 0 \dots k$ with $\mathbf{w}^0 = \mathbf{x}$ and 3-gon classes $\psi'_{g^i} \in \pi_2(\boldsymbol{\theta}_{\boldsymbol{\alpha}^{i-1}\boldsymbol{\alpha}^i}, \mathbf{w}^i, \mathbf{w}^{i-1})$ such that

$$\mu(\psi'_{g^i}) = 0 \quad \text{and} \quad [\psi'_{g^i}] \cdot [\bigtriangledown] = 0 \quad \text{for} \quad i = 1, \dots, k.$$

Now recall that via the ψ_{f^i} and ψ_{g^i} classes, the proof of part 1 of this lemma provides 2-gon classes $\phi^j \in \pi_2(\mathbf{w}^j, \mathbf{z}^j)$ with

$$\mu(\phi^j) = 0 \quad \text{and} \quad [\phi^j] \cdot [\bigtriangledown] \geq 0 \quad \text{for} \quad j = 1, \dots, k.$$

Notice that $\psi'_{g^1} + \zeta^0, \phi^1 + \zeta^1 + \psi_{h^1} \in \pi_2(\boldsymbol{\theta}_{\boldsymbol{\alpha}^0\boldsymbol{\alpha}^1}, \mathbf{w}^1, \mathbf{x})$. Then there is some 3-gon η^1 with triply-periodic domain such that

$$\psi'_{g^1} + \zeta^0 = \phi^1 + \zeta^1 + \psi_{h^1} + \eta^1.$$

Similarly, for each $i = 2, \dots, k$, there is a 3-gon η^i with triply-periodic domain such that

$$\psi'_{g^i} + \phi^{i-1} + \zeta^{i-1} = \phi^i + \zeta^i + \psi_{h^i} + \eta^i.$$

Taking intersections with the anti-diagonal $\bigtriangledown$ and recalling that $[\psi'_{g^j}] \cdot [\bigtriangledown] = [\eta^j] \cdot [\bigtriangledown] = 0$, we have that

$$\begin{aligned}
[\zeta^0] \cdot [\bigtriangledown] &= [\phi^1] \cdot [\bigtriangledown] + [\zeta^1] \cdot [\bigtriangledown] + [\psi_{h^1}] \cdot [\bigtriangledown] \\
&= [\phi^2] \cdot [\bigtriangledown] + [\zeta^2] \cdot [\bigtriangledown] + [\psi_{h^2}] \cdot [\bigtriangledown] + [\psi_{h^1}] \cdot [\bigtriangledown] \\
&= \dots = [\phi^k] \cdot [\bigtriangledown] + [\zeta^k] \cdot [\bigtriangledown] + \sum_{j=1}^{k} [\psi_{h^j}] \cdot [\bigtriangledown] \geq 0.
\end{aligned}$$

On the other hand, given some $\mathbf{z}, \mathbf{w} \in \mathbb{T}_{\boldsymbol{\alpha}'} \cap \mathbb{T}_{\boldsymbol{\beta}}$ such that $\mathbf{w}$ is a term in $G(\mathbf{z})$, a similar argument produces a 2-gon class $\xi^0 \in \pi_2(\mathbf{z}, \mathbf{w})$ such that $[\xi^0] \cdot [\bigtriangledown] \geq 0$. $\square$

Lemma 27. *Let $\mathcal{H}_{\boldsymbol{\alpha}\boldsymbol{\beta}} = (\Sigma; \boldsymbol{\alpha}; \boldsymbol{\beta}; z)$ and $\mathcal{H}_{\boldsymbol{\alpha}'\boldsymbol{\beta}'} = \big(\Sigma; \boldsymbol{\alpha}'; \boldsymbol{\beta}'; z\big)$ be two pointed Heegaard diagrams for the manifold $\Sigma(K)\#(S^2 \times S^1)$ which are obtained from braids b and b' via Theorem 21 (possibly after Heegaard stabilization), where*

$$\boldsymbol{\beta} = \boldsymbol{\beta}^0 \to \boldsymbol{\beta}^1 \to \ldots \to \boldsymbol{\beta}^n = \boldsymbol{\beta}' \quad \textit{and} \quad \boldsymbol{\alpha} = \boldsymbol{\alpha}^0 \to \boldsymbol{\alpha}^1 \to \ldots \to \boldsymbol{\alpha}^m = \boldsymbol{\alpha}'$$

are sequences of handleslides and isotopies. Also let $g = g^n_{\boldsymbol{\beta}} \circ \ldots \circ g^1_{\boldsymbol{\beta}} \circ g^m_{\boldsymbol{\alpha}} \circ \ldots \circ g^1_{\boldsymbol{\alpha}}$ be the composition of the α- and β-triangle injections

$$g^k_{\boldsymbol{\beta}} : \mathbb{T}_{\boldsymbol{\alpha}} \cap \mathbb{T}_{\boldsymbol{\beta}^{k-1}} \to \mathbb{T}_{\boldsymbol{\alpha}} \cap \mathbb{T}_{\boldsymbol{\beta}^k} \quad \textit{and} \quad g^k_{\boldsymbol{\alpha}} : \mathbb{T}_{\boldsymbol{\alpha}^{k-1}} \cap \mathbb{T}_{\boldsymbol{\beta}^n} \to \mathbb{T}_{\boldsymbol{\alpha}^k} \cap \mathbb{T}_{\boldsymbol{\beta}^n}$$

Let $f^k_{\boldsymbol{\alpha}}$ and $f^k_{\boldsymbol{\beta}}$ denote the chain homotopy equivalences induced by the $\boldsymbol{\alpha}$ and $\boldsymbol{\beta}$ moves and let $h^k_{\boldsymbol{\alpha}}$ and $h^k_{\boldsymbol{\beta}}$ denote their homotopy inverses. For the maps

$$f = f^n_{\boldsymbol{\beta}} \circ \ldots \circ f^1_{\boldsymbol{\beta}} \circ f^m_{\boldsymbol{\alpha}} \circ \ldots \circ f^1_{\boldsymbol{\alpha}} \quad \textit{and} \quad h = h^1_{\boldsymbol{\alpha}} \circ \ldots \circ h^m_{\boldsymbol{\alpha}} \circ h^1_{\boldsymbol{\beta}} \circ \ldots \circ h^n_{\boldsymbol{\beta}},$$

let $H : \widehat{CF}(\mathcal{H}_{\boldsymbol{\alpha}\boldsymbol{\beta}}) \to \widehat{CF}(\mathcal{H}_{\boldsymbol{\alpha}\boldsymbol{\beta}})$ and $G : \widehat{CF}(\mathcal{H}_{\boldsymbol{\alpha}'\boldsymbol{\beta}'}) \to \widehat{CF}(\mathcal{H}_{\boldsymbol{\alpha}',\boldsymbol{\beta}'})$ be the natural 4-gon-counting homotopies such that

$$hf - id_{\widehat{CF}(\mathcal{H}_{\boldsymbol{\alpha}\boldsymbol{\beta}})} = \widehat{\partial} H + H \widehat{\partial} \quad \textit{and} \quad fh - id_{\widehat{CF}(\mathcal{H}_{\boldsymbol{\alpha}'\boldsymbol{\beta}'})} = \widehat{\partial} G + G \widehat{\partial}.$$

Then for each torsion $\mathfrak{s} \in Spin^c(\Sigma(K)\#(S^2 \times S^1))$, the following hold:

(i) If $\mathbf{y} \in \mathbb{T}_{\boldsymbol{\alpha}'} \cap \mathbb{T}_{\boldsymbol{\beta}'}$ is a term in $f(\mathbf{x})$ for some $\mathbf{x} \in \mathfrak{U}_{\mathfrak{s}} \subset \mathbb{T}_{\boldsymbol{\alpha}} \cap \mathbb{T}_{\boldsymbol{\beta}}$ and if $\mathbf{w} \in \mathbb{T}_{\boldsymbol{\alpha}} \cap \mathbb{T}_{\boldsymbol{\beta}}$ is a term in $h(\mathbf{z})$ for some $\mathbf{z} \in \mathfrak{U}'_{\mathfrak{s}} \subset \mathbb{T}_{\boldsymbol{\alpha}'} \cap \mathbb{T}_{\boldsymbol{\beta}'}$, then

$$R(\mathbf{y}) \leq R(g(\mathbf{x})) \quad \textit{and} \quad R(\mathbf{z}) \geq R(g(\mathbf{w})).$$

(ii) If $\mathbf{y} \in \mathbb{T}_{\boldsymbol{\alpha}} \cap \mathbb{T}_{\boldsymbol{\beta}}$ is a term in the sum $H(\mathbf{x})$ for some $\mathbf{x} \in \mathfrak{U}_{\mathfrak{s}} \subset \mathbb{T}_{\boldsymbol{\alpha}} \cap \mathbb{T}_{\boldsymbol{\beta}}$ and if $\mathbf{w} \in \mathbb{T}_{\boldsymbol{\alpha}'} \cap \mathbb{T}_{\boldsymbol{\beta}'}$ is a term in the sum $G(\mathbf{z})$ for some $\mathbf{z} \in \mathfrak{U}'_{\mathfrak{s}} \subset \mathbb{T}_{\boldsymbol{\alpha}'} \cap \mathbb{T}_{\boldsymbol{\beta}'}$, then

$$\rho(\mathbf{y}) \leq \rho(\mathbf{x}) \quad \textit{and} \quad \rho(\mathbf{w}) \leq \rho(\mathbf{z}).$$

Proof of part 1. By a simple extension of the argument in the proof of part 1 of Lemma 26, one can find 2-gons $\phi \in \pi_2(g(\mathbf{x}), \mathbf{y})$ and $\phi' \in \pi_2(\mathbf{z}, g(\mathbf{w}))$ such that

$$\mu(\phi) = \mu(\phi') = 0, \quad [\phi] \cdot [\bigtriangledown] \geq 0, \quad \text{and} \quad [\phi'] \cdot [\bigtriangledown] \geq 0.$$

□

Proof of part 2. Extending the argument in the proof of part 2 of Lemma 26, one obtains 2-gons $\zeta \in \pi_2(\mathbf{x}, \mathbf{y})$ and $\xi \in \pi_2(\mathbf{z}, \mathbf{w})$ such that

$$[\zeta] \cdot [\bigtriangledown] \geq 0 \quad \text{and} \quad [\xi] \cdot [\bigtriangledown] \geq 0.$$

□

Lemma 28. *Let $\mathcal{H} = (\Sigma; \boldsymbol{\alpha}; \boldsymbol{\beta}; z)$ and $\mathcal{H}' = \left(\Sigma; \boldsymbol{\alpha}'; \boldsymbol{\beta}'; z\right)$ be two Heegaard diagrams for the manifold $\Sigma(K)\#(S^2 \times S^1)$ which are obtained from braids b and b' (possibly after Heegaard stabilization), and related by handleslides and isotopies in the sense of Lemma 26 or Lemma 27. Assume also that there are α- and β- triangle injections corresponding to each of these moves such that their composition*

$$g : \mathbb{T}_{\boldsymbol{\alpha}} \cap \mathbb{T}_{\boldsymbol{\beta}} \to \mathbb{T}_{\boldsymbol{\alpha}'} \cap \mathbb{T}_{\boldsymbol{\beta}'}$$

satisfies $R(g(\mathbf{x})) = R(\mathbf{x})$ for all $\mathbf{x} \in \mathbb{T}_{\boldsymbol{\alpha}} \cap \mathbb{T}_{\boldsymbol{\beta}}$. Then for each $\mathfrak{s} \in Spin^c(\Sigma(K)\#(S^2 \times S^1))$ torsion, the following hold:

(i) The composition $f : \widehat{CF}(\mathcal{H}, \mathfrak{s}) \to \widehat{CF}(\mathcal{H}', \mathfrak{s})$ of chain homotopy equivalences induced by the moves and its homotopy inverse $h : \widehat{CF}(\mathcal{H}', \mathfrak{s}) \to \widehat{CF}(\mathcal{H}, \mathfrak{s})$ are ρ-filtered chain maps.

(ii) The homotopies H from $g \circ f$ to $id_{\widehat{CF}(\mathcal{H}, \mathfrak{s})}$ and H' from $f \circ g$ to $id_{\widehat{CF}(\mathcal{H}', \mathfrak{s})}$ are ρ-filtered chain homotopies.

In particular, the ρ-filtered complexes $\widehat{CF}(\mathcal{H}, \mathfrak{s})$ and $\widehat{CF}(\mathcal{H}', \mathfrak{s})$ have the same filtered chain homotopy type.

Proof of part 1. Let $\mathbf{y} \in \mathbb{T}_{\boldsymbol{\alpha}'} \cap \mathbb{T}_{\boldsymbol{\beta}'}$ be a term in the sum $f(\mathbf{x})$, where $\mathbf{x} \in \mathfrak{U}_{\mathfrak{s}} \subset \mathbb{T}_{\boldsymbol{\alpha}} \cap \mathbb{T}_{\boldsymbol{\beta}}$. By Lemma 26 or 27, the assumption that g preserves the R-grading, and the fact that the chain map induced by a handleslide preserves $\widetilde{gr}$,

$$\rho(\mathbf{x}) = R(\mathbf{x}) - \widetilde{gr}(\mathbf{x}) = R(g(\mathbf{x})) - \widetilde{gr}(\mathbf{x}) \geq R(\mathbf{y}) - \widetilde{gr}(\mathbf{x}) = R(\mathbf{y}) - \widetilde{gr}(\mathbf{y}) = \rho(\mathbf{y}).$$

Analogously, $\rho(\mathbf{z}) \geq \rho(\mathbf{w})$ for every term $\mathbf{w}$ sum $h(\mathbf{z})$, where $\mathbf{z} \in \mathfrak{U}'_{\mathfrak{s}} \subset \mathbb{T}_{\boldsymbol{\alpha}'} \cap \mathbb{T}_{\boldsymbol{\beta}'}$. □

Proof of part 2. This is just a restatement of part 2 of Lemma 26 or 27. □

Remark 29. We will use a slightly modified version of Lemma 28 in Section **??**. In particular, we can obtain an analogous result when $\boldsymbol{\alpha}$ (respectively $\boldsymbol{\beta}$) and $\boldsymbol{\alpha}'$ (respectively $\boldsymbol{\beta}'$) are related by many handleslides and isotopies, but we only have one $\boldsymbol{\alpha}$-triangle injection $g_{\boldsymbol{\alpha}} : \mathbb{T}_{\boldsymbol{\alpha}} \cap \mathbb{T}_{\boldsymbol{\beta}} \to \mathbb{T}_{\boldsymbol{\alpha}'} \cap \mathbb{T}_{\boldsymbol{\beta}}$ and one $\boldsymbol{\beta}$-triangle injection $g_{\boldsymbol{\beta}} : \mathbb{T}_{\boldsymbol{\alpha}'} \cap \mathbb{T}_{\boldsymbol{\beta}} \to \mathbb{T}_{\boldsymbol{\alpha}'} \cap \mathbb{T}_{\boldsymbol{\beta}'}$. Let

$$\boldsymbol{\alpha} = \boldsymbol{\alpha}^0 \to \boldsymbol{\alpha}^1 \to \ldots \to \boldsymbol{\alpha}^n = \boldsymbol{\alpha}'$$

be the sequence of handleslides and isotopies, and let $\psi_k \in \pi_2(\boldsymbol{\theta}_{\boldsymbol{\alpha}^k \boldsymbol{\alpha}^{k-1}}, \mathbf{x}_{k-1}, \mathbf{x}^k)$ be a 3-gon with pseudo-holomorphic representative such that $\mu(\psi_k) = 0$. Then there is a 3-gon class $\psi \in \pi_2(\boldsymbol{\theta}_{\boldsymbol{\alpha}'\boldsymbol{\alpha}}, \mathbf{x}_0, \mathbf{x}^n)$ with $\mu(\psi) = 0$ and $[\psi] \cdot [\bigtriangledown] \geq 0$. This 3-gon class ψ is the one we should compare with the class ψ^+ associated to $g_{\boldsymbol{\alpha}}$.

We turn to a few lemmas which will later allow us to restrict our attention to multiplication of braids in B_{2n} by elements of K_{2n} on the right side only. Notice first that the symplectic automorphism induced by the braid $b \in B_{2n}$ on the punctured disk induces a symplectic automorphism.

$$f_b : Sym^n(\Sigma) \to Sym^n(\Sigma)$$

One can see that there is an induced graded symplectic automorphism $\widetilde{f_b}$ with respect to gradings provided by the volume form.

Lemma 30. *Let $f_b : Sym^n(\Sigma) \to Sym^n(\Sigma)$ be the automorphism discussed above and let $\bigtriangledown \subset Sym^n(\Sigma)$ denote the anti-diagonal. Then $f_b(\bigtriangledown) = \bigtriangledown$.*

Proof. Let $\mathbf{x} \in \bigtriangledown$. Then $\mathbf{x}$ contains components (u_1, z_1) and (u_2, z_2) such that $z_2 = z_1$ and $u_2 = -u_1$. Suppose that $u_2 \neq 0$. Then $f_b(\mathbf{x}) = (v_k, w_k)$ contains components $(v_1, w_1) = f_b(u_1, z_1)$ and $(v_2, w_2) = f_b(u_2, z_2)$. Since f is induced by a map on the punctured disk, we have that $w_2 = w_1$. Therefore, $(v_2)^2 = (v_1)^2$ and so $v_2 = \pm v_1$.

Now $\mathbf{x}' = (u'_k, z'_k) \in \Delta$ be such that $u'_2 = -u_2$, $u'_j = u_j$ for $j \neq 2$, and $z'_j = z_j$ for $j = 1, \dots, n$. Then if $f_b(\mathbf{x}') = (v'_k, w'_k)$, we then have that $v'_j = v_j$ for $j \neq 2$ and $w'_j = w_j$ for $j = 1, \dots, n$. Further, $v'_2 = v'_1 = v_1 = \pm v_2$. But $\mathbf{x} \neq \mathbf{x}'$, so $v'_2 \neq v_2$ and thus $v_2 = -v_1$.

Now suppose that $u_2 = u_1 = 0$. Then z_2 is a puncture point. However, a braid element diffeomorphism on the punctured disk fixes the set of punctures, and so $v_2 = v_1 = 0$ also. So, $f_b(\mathbf{x}) \in \bigtriangledown$ in this case also.

One can similarly show that $f_b^{-1}(\bigtriangledown) \subset \bigtriangledown$. □

As shorthand, let $\widetilde{f}_b(\mathbb{T}_{\boldsymbol{\alpha}})$ be denoted by $b\mathbb{T}_{\boldsymbol{\alpha}}$ from now on. Since R provides an absolute grading on $CF_*(\mathbb{T}_{\boldsymbol{\alpha}}, b\mathbb{T}_{\boldsymbol{\alpha}})$, when computed inside $Sym^n(\Sigma) - \bigtriangledown$, then one can define a grading R^* on $CF^{-*}(\mathbb{T}_{\boldsymbol{\alpha}}, b\mathbb{T}_{\boldsymbol{\alpha}})$ via

$$R^*(\mathbf{x}^*) = -R(\mathbf{x}) \quad \text{for each } \mathbf{x} \in \mathbb{T}_{\boldsymbol{\alpha}} \cap b\mathbb{T}_{\boldsymbol{\alpha}}.$$

Lemma 31. *Let $b \in B_{2n}$ be a braid. Then when computed inside $Sym^n(\Sigma) - \bigtriangledown$,*

$$CF_*(\mathbb{T}_{\boldsymbol{\alpha}}, b\mathbb{T}_{\boldsymbol{\alpha}}) \quad \text{and} \quad CF^{-*}\left(\mathbb{T}_{\boldsymbol{\alpha}}, b^{-1}\mathbb{T}_{\boldsymbol{\alpha}}\right)$$

are isomorphic as absolutely graded chain complexes equipped with the gradings R and R^*, respectively.

Proof. Well, we have that the grading $\widetilde{R}$ arises as an absolute grading induced by gradings on totally-real submanifolds, and so as $\widetilde{R}$-graded complexes,

$$CF_*(\mathbb{T}_{\boldsymbol{\alpha}}, b\mathbb{T}_{\boldsymbol{\alpha}}) \cong CF^{n-*}(b\mathbb{T}_{\boldsymbol{\alpha}}, \mathbb{T}_{\boldsymbol{\alpha}}) \cong CF^{n-*}\left(\mathbb{T}_{\boldsymbol{\alpha}}, b^{-1}\mathbb{T}_{\boldsymbol{\alpha}}\right).$$

But since $s_R(b^{-1}) + s_R(b) = -n$, the result follows. □

When one computes these complexes inside all of $Sym^n(\Sigma)$, recall that

$$CF^{-*}(\mathbb{T}_{\boldsymbol{\alpha}}, b\mathbb{T}_{\boldsymbol{\alpha}}) = \widehat{CF}(\mathcal{H}_b),$$

where $\mathcal{H}_b$ is the admissible Heegaard diagram for $\Sigma(K)\#(S^2 \times S^1)$ provided by Proposition 21 and K is the closure of b. It is clear that R^* provides a filtration on this complex.

Lemma 32. *Let $b \in B_{2n}$ be a braid and denote by $\mathcal{H}_b$ and $\mathcal{H}_{b^{-1}}$ the admissible Heegaard diagrams induced by the braid b and b^{-1}, respectively. Then*

$$\widehat{CF}_*(\mathcal{H}_{b^{-1}}) \quad \text{and} \quad \widehat{CF}^{-*}(\mathcal{H}_b)$$

are isomorphic as filtered chain complexes equipped with the filtrations R and R^*, respectively.

Proof. When one extends the computation of the Floer complexes to all of $Sym^n(\Sigma)$, the differentials may have additional terms which count classes of 2-gons intersecting $\bigtriangledown$. By Lemma 30, the chain isomorphisms in the proof of Lemma 31 induce identifications between such classes which preserve intersection counts with $\bigtriangledown$. □

Now given a braid word $b = \sigma_{i_1}^{k_1} \dots \sigma_{i_m}^{k_m} \in B_{2n}$, let $-b$ denote the braid word

$$-b = \sigma_{2n-i_1}^{-k_1} \dots \sigma_{2n-i_m}^{-k_m} \in B_{2n}.$$

Lemma 33. *Let $b \in B_{2n}$ be a braid whose closure is the knot K, let $\mathfrak{s} \in Spin^c(\Sigma(K)\#(S^2 \times S^1))$ be torsion, and denote by $\mathcal{H}_b$ and $\mathcal{H}_{-b}$ the admissible Heegaard diagrams induced by the braids b and $-b$, respectively. Then*

$$\widehat{CF}_*(\mathcal{H}_b, \mathfrak{s}) \quad \text{and} \quad \widehat{CF}^{-*}(\mathcal{H}_{-b}, \mathfrak{s})$$

are isomorphic as filtered chain complexes equipped with the filtrations R and R^*, respectively.

Proof. Let $\mathcal{F}^+$ and $\mathcal{F}^-$ be the fork diagrams induced by b and $-b$, respectively. Notice that if the closure of b is the knot K, then the closure of $-b$ is $-K$, the mirror image of K. Therefore, $\mathcal{H}_{\pm b}$ is a Heegaard diagram for $\pm\Sigma(K)\#(S^2 \times S^1)$. Let $\iota : \mathbb{C} \to \mathbb{C}$ be the map given by $z \mapsto -\overline{z}$, and let $\widetilde{\mathcal{F}}$ denote the "fork-like" diagram obtained by applying ι to $\mathcal{F}^+$. Notice that if one ignores the handles, then $\widetilde{\mathcal{F}}$ is isotopic to $\mathcal{F}^-$. Figure 13 compares local pictures of these diagrams.

This map induces a diffeomorphism $\widehat{\iota} : \Sigma \to -\Sigma$, where $\mathcal{H}_b = (\Sigma, \boldsymbol{\alpha}, \boldsymbol{\beta}, +\infty)$ and $\mathcal{H}_{-b} = (-\Sigma, \boldsymbol{\alpha}, \boldsymbol{\beta}, +\infty)$. Recall that for any closed, connected, oriented 3-manifold Y, $\mathrm{Spin}^c(Y) \cong \mathrm{Spin}^c(-Y)$. For each torsion $\mathfrak{s} \in \mathrm{Spin}^c(\Sigma(K)\#(S^2 \times S^1))$, Ozsváth and Szabó described in [9] a natural chain isomorphism

$$\Phi : \widehat{CF}_*(\Sigma(-K)\#(S^2 \times S^1), \mathfrak{s}) \to \widehat{CF}^{-*}(\Sigma(K)\#(S^2 \times S^1), \mathfrak{s}),$$

which in our case is realized by $\Phi(\mathbf{x}) = \left(\{\widehat{\iota}^{-1}(x_i)\}\right)^*$ for each generator $\mathbf{x}$ for $\widehat{CF}_*(\Sigma(-K)\#(S^2 \times S^1), \mathfrak{s})$.

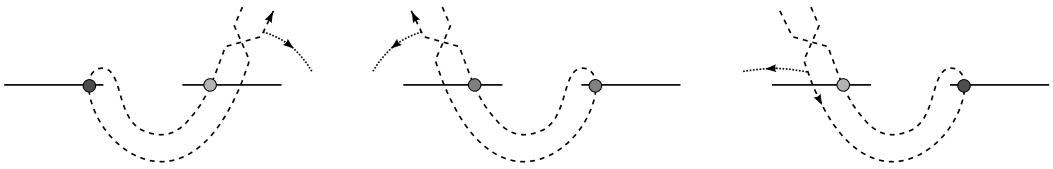

(a) The diagram $\mathcal{F}^+$ for K (b) $\widetilde{\mathcal{F}}$, the mirror image of $\mathcal{F}^+$ (c) The diagram $\mathcal{F}^-$ for $-K$

Figure 13: Local pictures of fork diagrams, where corresponding points are marked with matching dots

Figure 13 displays a suitably general local picture of the fork diagrams involved. Let $\mathbf{z}^+$ be a generator in $\mathcal{F}^+$, let $\widetilde{\mathbf{z}}$ be the tuple in $\widetilde{\mathcal{F}}$ such that $\widetilde{z}_j = \iota(z_j^+)$, and let $\mathbf{z}^-$ be the corresponding generator in $\mathcal{F}^-$. Define the functions Q, P, T, and $\widetilde{R}$ on $\widetilde{\mathcal{F}}$ in the obvious way. One can verify that

$$(P^* - Q^*)(z_j^-) = (P^* - Q^*)(\widetilde{z}_j) + 1 = -(P^* - Q^*)(z_j^+) + 1,$$
$$\text{and so} \quad (P - Q)(\mathbf{z}^-) = -(P - Q)(\mathbf{z}^+) + n.$$

Furthermore, $T(\mathbf{z}^-) = -T(\mathbf{z}^+)$, and

$$s_R(b^-, D^-) = \frac{e(b^-) - w(D^-) - 2n}{4} = \frac{-e(b^+) + w(D^+) - 2n}{4}$$
$$= -\frac{e(b^+) - w(D^+) - 2n}{4} - n.$$

Therefore, we have that $R(\mathbf{z}^-) = -R(\mathbf{z}^+)$, and so both Φ and Φ^{-1} are filtered. □

5.1 Fork diagram isotopy

The identification of a braid b with its associated fork diagram is only defined upto isotopy of the fork diagram. We should verify the following:

Proposition 34. *Let $\mathfrak{s} \in Spin^c(\Sigma(K)\#(S^2 \times S^1))$ be torsion. Then the ρ-filtered chain homotopy type of $\widehat{CF}(\Sigma(K)\#(S^2 \times S^1), \mathfrak{s})$ is an invariant of the braid b.*

Remark 35. The reader should note that in the original proof in [10] of the invariance of the group $\widehat{HF}(M)$ under isotopies of the Heegaard diagram for M, pseudo-holomorphic 3-gons were not used. Lipshitz observed in [6] that the induced chain map could be defined in terms of counting 3-gons.

Proof. We omit explicit analysis of isotopies which don't introduce or annihilate intersection points between α and β arcs (i.e. preserve $\mathcal{Z}$ and $\mathcal{G}$); these just induce intersection-preserving isotopies on the Heegaard diagram. However, we should verify invariance under the type of isotopy shown in Figure 14.

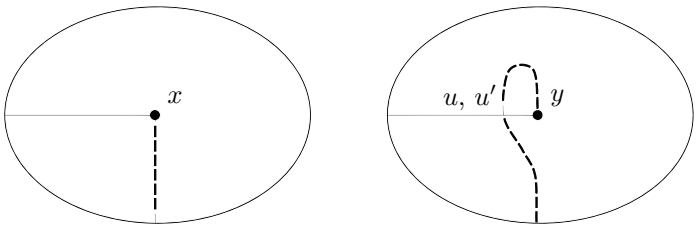

(a) Before isotopy (b) After isotopy

Figure 14: Introducing new intersections via an isotopy

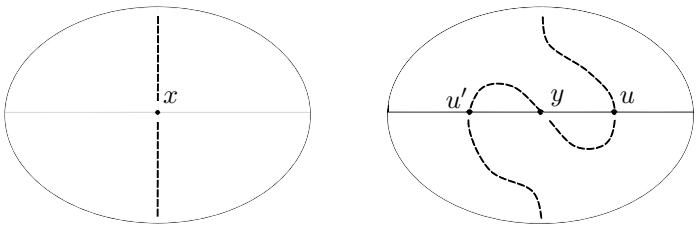

(a) Before isotopy (b) After isotopy

Figure 15: Isotopic Heegaard diagrams for $\Sigma(K)\#(S^2 \times S^1)$ covering the fork diagrams in Figure 14

Taking the two-fold cover of this local fork diagram branched on the one puncture gives the local Heegaard diagrams for $\Sigma(K)\#(S^2 \times S^1)$ shown in Figure 15. The isotopy on the fork diagram

amounts to an isotopy on the Heegaard diagram, and by Lemma 28 it is sufficient to construct a $\boldsymbol{\beta}$-triangle injection g_{iso} and check that it preserves R.

We see from the 3-sided region in Figure 16 that we can define the injection g_{iso} such that $g_{iso}(x\mathbf{z}) = u\mathbf{z}$. Further, the loops in Figure 17 show that $Q^*(u) = Q^*(x)$, $P^*(u) = P^*(x)$, and $T(u\mathbf{z}) = T(x\mathbf{z})$. Therefore, $R(u\mathbf{z}) = R(x\mathbf{z})$. □

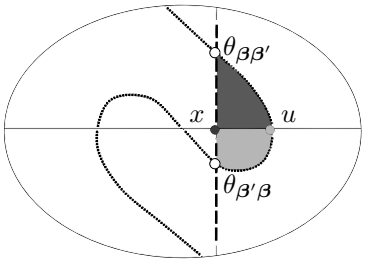

Figure 16: Local regions in domains of the 3-gons $\psi^+_{g_{iso}}$ (dark gray) and $\psi^-_{g_{iso}}$ (light gray)

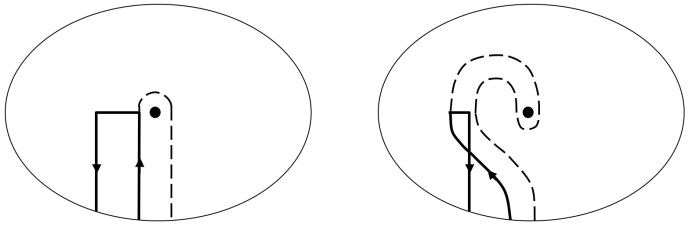

(a) x (b) u

Figure 17: Loops used to compute gradings for x and u

5.2 Invariance under choice of braid

Proof of Theorem 1. It suffices to verify that if b and b' (inducing Heegaard diagrams $\mathcal{H}$ and $\mathcal{H}'$ for $\Sigma(K)\#(S^2 \times S^1)$) are related by a Birman move, then the ρ-filtered complexes $\widehat{CF}(\mathcal{H}, \mathfrak{s})$ and $\widehat{CF}(\mathcal{H}', \mathfrak{s})$ have the same filtered chain homotopy type for each torsion $\mathfrak{s} \in \mathrm{Spin}^c(\Sigma(K)\#(S^2 \times S^1))$.

We first claim that we don't need to explicitly examine Birman moves of the form $b \mapsto gb$, where $b \in B_{2n}$ and $g \in K_{2n}$. Well, by Lemmas 32 and 33, the R-filtered complexes

$$\widehat{CF}_*(\mathcal{H}_{gb}, \mathfrak{s}) \quad \text{and} \quad \widehat{CF}_*(\mathcal{H}_{bf}, \mathfrak{s})$$

are filtered chain isomorphic, where $f = -g^{-1}$. We won't explicitly analyze moves of the form $b \mapsto b(-g)$ for generators g of K_{2n}, but the local pictures would be mirror images of those for $b \mapsto bg$ and the arguments would be completely analogous.

We'll see that each Birman move induces either a diffeomorphism of the Heegaard surface or a sequence of isotopies and handleslides relating Heegaard diagrams for $\Sigma(K)\#(S^2 \times S^1)$ induced by the fork diagrams before and after the move (also preceded by a Heegaard stabilization in the Birman stabilization move).

For the case of a surface diffeomorphism, one obtains a chain complex isomorphism which will be shown to preserve R. By Lemma 30, such an isomorphism also preserves the filtration ρ.

We saw in Section 2.1 that isotopies and handleslides on Heegaard diagrams induce chain homotopy equivalences on $\widehat{CF}(\Sigma(K)\#(S^2 \times S^1))$ which count pseudo-holomorphic 3-gon classes of

index zero. For each isotopy or handleslide taking $\boldsymbol{\alpha}$ and $\boldsymbol{\beta}$ to $\boldsymbol{\alpha}'$ and $\boldsymbol{\beta}'$, we'll define a triangle injection $g : \mathbb{T}_{\boldsymbol{\alpha}} \cap \mathbb{T}_{\boldsymbol{\beta}} \hookrightarrow \mathbb{T}_{\boldsymbol{\alpha}'} \cap \mathbb{T}_{\boldsymbol{\beta}'}$. By Lemma 28, it suffices to construct these injections g and verify that $R(g(\mathbf{x})) = R(\mathbf{x})$ for each $\mathbf{x} \in \mathcal{G}$. Notice that since the moves induce local changes only, we'll only demonstrate local regions in the domains of the 3-gons lying in neighborhoods of the moves. We exhibit such domains and check gradings in Section 5.3. □

5.3 Local effects of Birman moves

5.3.1 $b \mapsto bA^{\pm 1} = b\sigma_1^{\pm 1}$

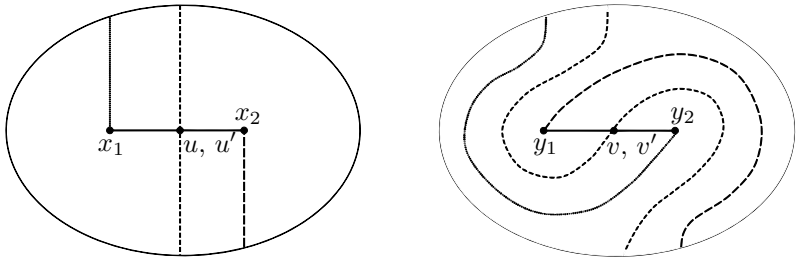

(a) Local diagram for b (b) Local diagram for bA

Figure 18: Fork diagrams associated to the move $b \mapsto bA$

The fork diagrams for $b \mapsto bA$ can be seen in Figure 18. This move induces a diffeomorphism on the Heegaard surface for $\Sigma(K)\#(S^2 \times S^1)$ (in fact, a single Dehn twist) which sends $x_i \mapsto y_i$ for $i = 1, 2$ and sends $\{u, u'\} \hookrightarrow \{v, v'\}$. One thus obtains a chain isomorphism g_A on Heegaard Floer complexes, and we verify that for each $\mathbf{w} \in \mathcal{G}$, $R(g_A(\mathbf{w})) = R(\mathbf{w})$.

Figure 19 illustrates the loops in our local fork diagram associated to affected elements of $\mathcal{Z}$. Since R is stable, we only need to examine one $\mathcal{Z}$ representative for each element of $\widetilde{\mathcal{Z}} - \tau$.

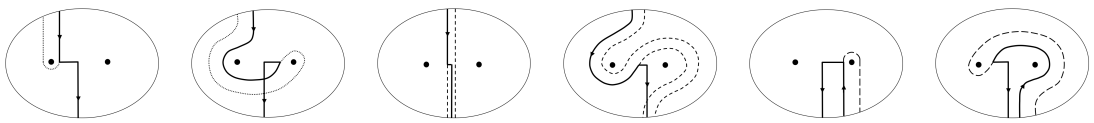

(a) x_1 (b) y_2 (c) u (d) v' (e) x_2 (f) y_1

Figure 19: Loops associated to elements of $\mathcal{Z}$ affected by $b \mapsto bA$

One can see that

$$Q(g_A(\mathbf{w})) = Q(\mathbf{w}) + 1 \quad \text{and} \quad P(g_A(\mathbf{w})) = P(\mathbf{w}) + 1 \quad \text{for all} \quad \mathbf{w} \in \mathcal{G}.$$

Since moves are local and at most one component is modified, T is preserved. The number of strands n is also preserved, but ϵ and w each increase by 1. So, $s_R(bA) = s_R(b)$, and

$$R(g_A(\mathbf{w})) = R(\mathbf{w}) \quad \text{for all} \quad \mathbf{w} \in \mathcal{G}.$$

The details for the move $b \mapsto bA^{-1}$ are analogous.

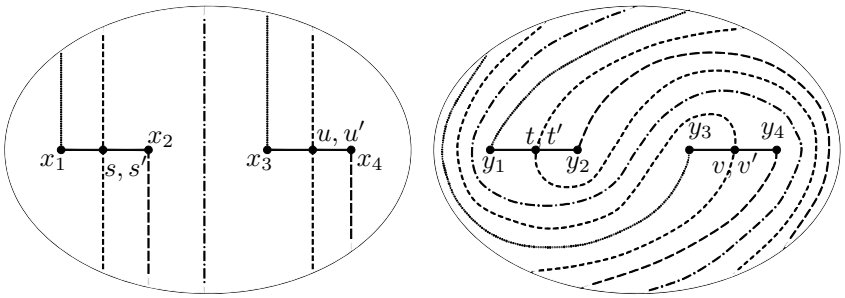

(a) Local diagram for b. (b) Local diagram for bC_i

Figure 20: Fork diagrams associated to $b \mapsto bC_i$

5.3.2 $b \mapsto bC_i^{\pm 1} = b\left(\sigma_{2i}\sigma_{2i-1}\sigma_{2i+1}\sigma_{2i}\right)^{\pm 1}$

This move induces a sequence of two Dehn twists, mapping intersections via

$$x_1 \mapsto y_3, \quad x_2 \mapsto y_4, \quad x_3 \mapsto y_1, \quad x_4 \mapsto y_2, \quad \{s, s'\} \hookrightarrow \{v, v'\} \quad \{u, u'\} \hookrightarrow \{t, t'\}.$$

We check that R is preserved by the induced chain isomorphism g_{C_i}.

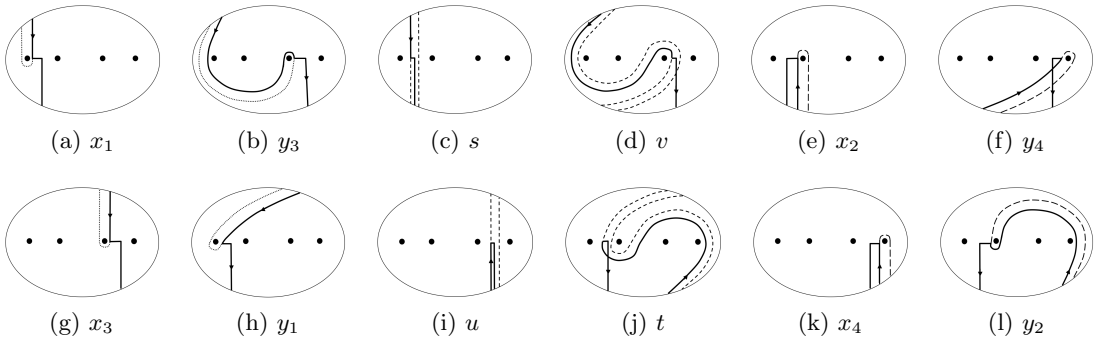

(a) x_1 (b) y_3 (c) s (d) v (e) x_2 (f) y_4

(g) x_3 (h) y_1 (i) u (j) t (k) x_4 (l) y_2

Figure 21: Loops associated to elements of $\mathcal{Z}$ affected by $b \mapsto bC_i$

We see from Figure 21 that for each $\mathbf{w} \in \mathcal{G}$,

$$Q(g_{C_i}(\mathbf{w})) = Q(\mathbf{w}) + 2, \quad P(g_{C_i}(\mathbf{w})) = P(\mathbf{w}), \quad \text{and} \quad T(g_{C_i}(\mathbf{w})) = T(\mathbf{w}) + 1.$$

Here n and w are unchanged, but ϵ increases by 4. So, $s_R(bC_i) = s_R(b) + 1$, and thus

$$R(g_{C_i}(\mathbf{w})) = R(\mathbf{w}) \quad \text{for all} \quad \mathbf{w} \in \mathcal{G}.$$

The proof associated to the move $b \mapsto bC_i^{-1}$ is analogous.

5.3.3 $b \mapsto bB^{\pm 1} = b\left(\sigma_2\sigma_1^2\sigma_2\right)^{\pm 1}$

The fork diagrams before and after this move can be seen in Figure 22. To better understand the fork diagram for bB, we perform the isotopy resulting in Figure 22c.

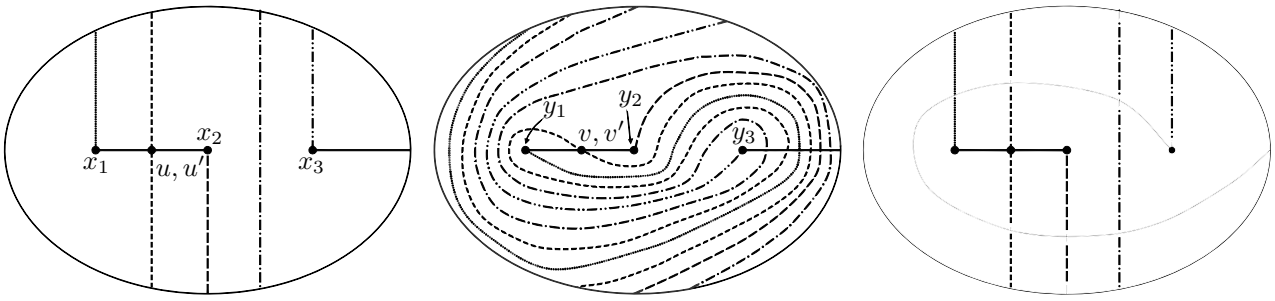

(a) Local diagram for b (b) Local diagram for bB (c) Isotopic to Figure 22b

Figure 22: Fork diagrams associated to $b \mapsto bB$

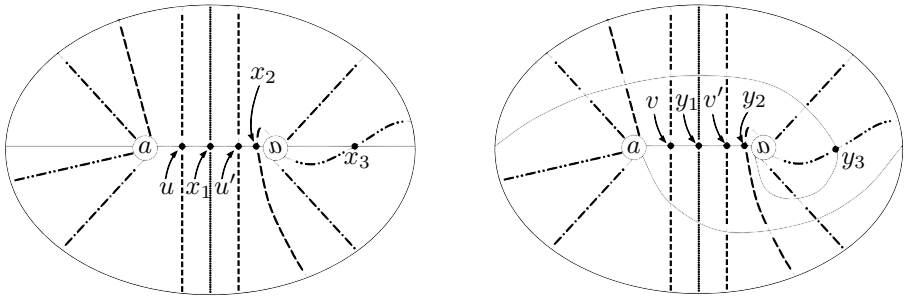

(a) From b (b) From bB

Figure 23: Heegaard diagrams for $\Sigma(K)\#(S^2 \times S^1)$ covering the fork diagrams in Figure 22

It is clear that only α_2 is altered by the move. To be more precise, we take a look at the Heegaard diagrams for $\Sigma(K)\#(S^2 \times S^1)$ which are the branched double-covers of the fork diagrams for b and bB. These can be seen in Figure 23.

To get from the left diagram to the right, we can perform a sequence of two handleslides; handleslide α_2 over α_1 to obtain α_2'', and then handleslide α_2'' over α_1 to obtain α_2'. Figure 24 details the two slides.

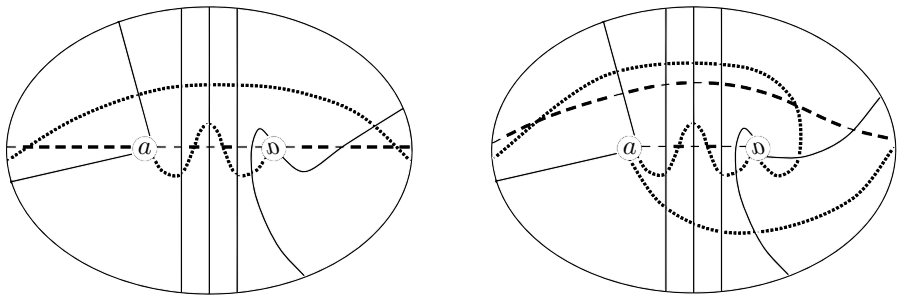

(a) $\boldsymbol{\alpha}$ (dotted) $\mapsto$ $\boldsymbol{\alpha}''$(dashed) (b) $\boldsymbol{\alpha}''$ (dotted) $\mapsto$ $\boldsymbol{\alpha}'$(dashed)

Figure 24: Two handleslides connecting Heegaard diagrams for b and bB

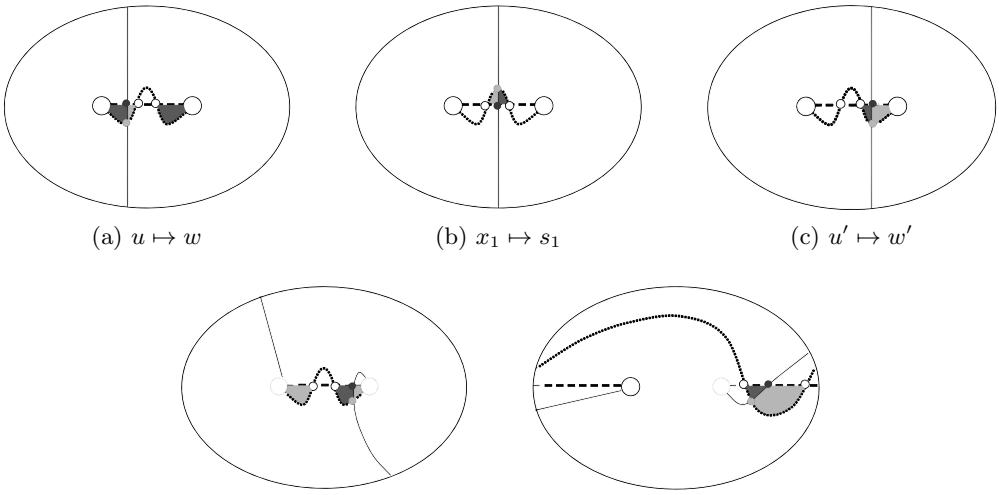

(a) $u \mapsto w$ (b) $x_1 \mapsto s_1$ (c) $u' \mapsto w'$

(d) $x_2 \mapsto s_2$ (e) $x_3 \mapsto s_3$

Figure 25: Local regions in domains of 3-gons ψ^+ (dark gray) and ψ^- (light gray) for g_B^a. White dots are components of $\boldsymbol{\theta}_{\boldsymbol{\alpha}''\boldsymbol{\alpha}}, \boldsymbol{\theta}_{\boldsymbol{\alpha}\boldsymbol{\alpha}''} \in \mathbb{T}_{\boldsymbol{\alpha}} \cap \mathbb{T}_{\boldsymbol{\alpha}''}$.

Let the injection g_B act as follows:

$$\begin{array}{cccc} x_1x_3\mathbf{y} \mapsto y_1y_3\mathbf{y}, & x_2x_3\mathbf{y} \mapsto y_2y_3\mathbf{y}, & ux_3\mathbf{y} \mapsto vy_3\mathbf{y}, & u'x_3\mathbf{y} \mapsto v'y_3\mathbf{y}, \\ x_1\mathbf{z} \mapsto y_1\mathbf{z}, & x_2\mathbf{z} \mapsto y_2\mathbf{z}, & u\mathbf{z}, \mapsto v\mathbf{z}, & u'\mathbf{z}, \mapsto v'\mathbf{z}. \end{array}$$

Note that $\mathbf{z}$ is an $(n-1)$-tuple whose component on the α_2 arc is not shown in the local fork diagram.

When viewed as a function on $\mathbb{T}_{\boldsymbol{\alpha}} \cap \mathbb{T}_{\boldsymbol{\beta}}$, g_B is a composition $g_B^a \circ g_B^b$ of triangle injections corresponding to the two handleslides. Local regions in domains of 3-gons for g_B^a and g_B^b can be seen in Figures 25 and 26, respectively. One can verify that if two of these regions appear in the domain of a 3-gon associated with g_B^a, then there are neighborhoods of these regions which map to disjoint neighborhoods in the fork diagram downstairs (and likewise for those associated with g_B^b). As a result, all 3-gons presented here avoid the anti-diagonal $\bigtriangledown$.

We see from Figure 27 that

$$\begin{array}{lll} Q(y_1y_3\mathbf{y}) = Q(x_1x_3\mathbf{y}) + 3, & Q(vy_3\mathbf{y}) = Q(ux_3\mathbf{y}) + 3, & Q(y_1\mathbf{z}) = Q(x_1\mathbf{z}) + 1, \\ Q(y_2y_3\mathbf{y}) = Q(x_2x_3\mathbf{y}) + 3, & Q(y_2\mathbf{z}) = Q(x_2\mathbf{z}) + 1, & Q(v\mathbf{z}) = Q(u\mathbf{z}) + 1, \end{array}$$

and

$$P(g_B(\mathbf{w})) = P(\mathbf{w}) \quad \text{for all} \quad \mathbf{w} \in \mathcal{G}.$$

Furthermore, one can check that

$$\begin{array}{lll} T(y_1y_3\mathbf{y}) = T(x_1x_3\mathbf{y}) + 2, & T(vy_3\mathbf{y}) = T(ux_3\mathbf{y}) + 2, & T(y_1\mathbf{z}) = T(x_1\mathbf{z}), \\ T(y_2y_3\mathbf{y}) = T(x_2x_3\mathbf{y}) + 2, & T(y_2\mathbf{z}) = T(x_2\mathbf{z}), & T(v\mathbf{z}) = T(u\mathbf{z}). \end{array}$$

This move preserves n and w, but increases ϵ by 4. Thus $s_R(bB) = s_R(b) + 1$, and

$$R(g_B(\mathbf{w})) = R(\mathbf{w}) \quad \text{for all} \quad \mathbf{w} \in \mathcal{G}.$$

The proof associated to the move $b \mapsto bB^{-1}$ is analogous.

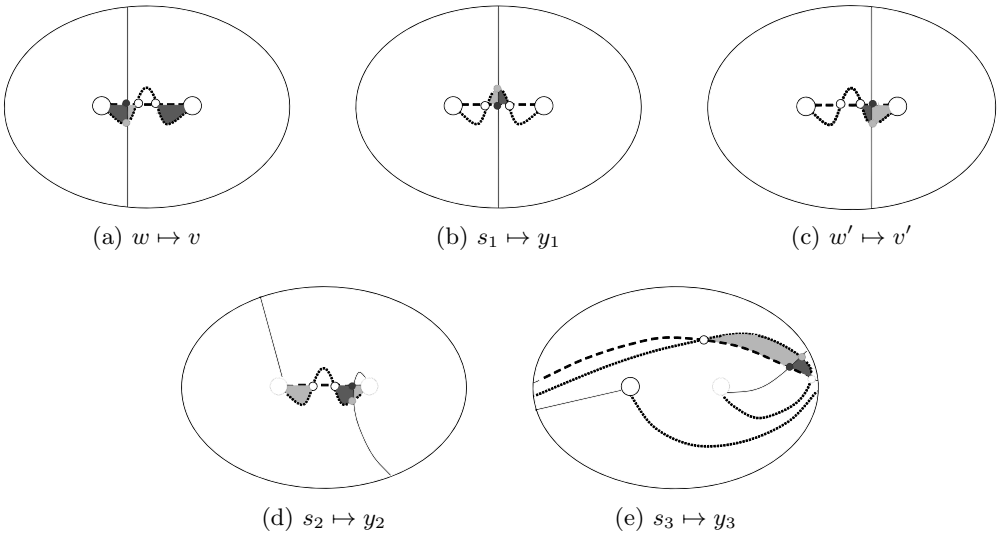

(a) $w \mapsto v$ (b) $s_1 \mapsto y_1$ (c) $w' \mapsto v'$

(d) $s_2 \mapsto y_2$ (e) $s_3 \mapsto y_3$

Figure 26: Local regions in domains of 3-gons ψ^+ (dark gray) and ψ^- (light gray) for g_B^b. White dots are components of $\boldsymbol{\theta}_{\boldsymbol{\alpha}'\boldsymbol{\alpha}''}, \boldsymbol{\theta}_{\boldsymbol{\alpha}''\boldsymbol{\alpha}'} \in \mathbb{T}_{\boldsymbol{\alpha}''} \cap \mathbb{T}_{\boldsymbol{\alpha}'}$.

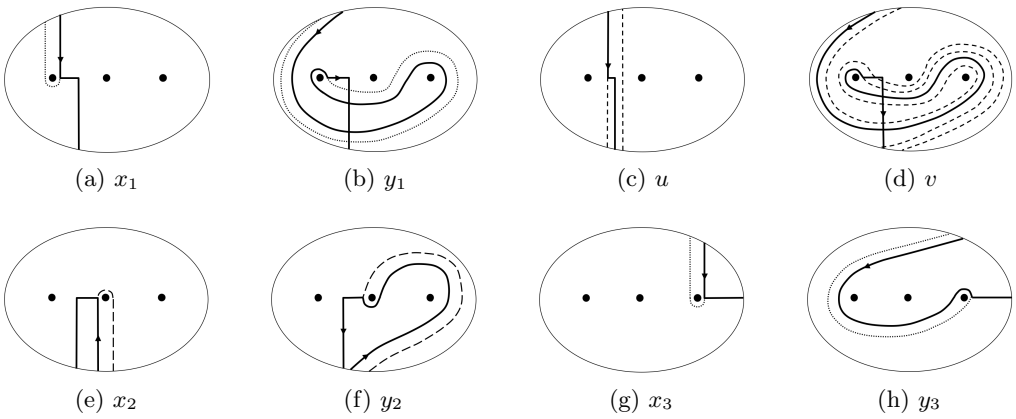

(a) x_1 (b) y_1 (c) u (d) v

(e) x_2 (f) y_2 (g) x_3 (h) y_3

Figure 27: Loops associated to elements of $\mathcal{Z}$ affected by $b \mapsto bB$

5.3.4 $b \in B_{2n} \leftrightarrow b\sigma_{2n} \in B_{2n+2}$

Fork diagrams before and after stabilization can be seem in Figure 28, and the induced Heegaard diagrams in Figure 29.

The stabilization braid move is a stabilization followed by several handleslides on the Heegaard diagram, two of which are relevant to our analysis and are seen in Figure 30. The destabilization braid move induces the inverse of this sequence of Heegaard moves.

Let x_{2n+1} denote the additional intersection obtained via Heegaard stabilization. We define the injection g_{stab} as follows

$$x_{2n}x_{2n+1}\mathbf{v} \mapsto y_{2n+1}y_{2n}\mathbf{v}, \quad x_{2n+1}\mathbf{z} \mapsto y_{2n+2}\mathbf{z},$$

where $\mathbf{v}$ is an $(n-1)$-tuple not contained in the local picture, and $\mathbf{z}$ is an n-tuple not contained

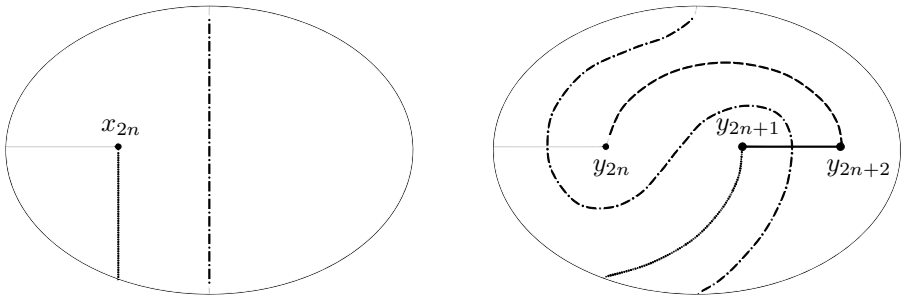

(a) Local diagram for $b \in B_{2n}$ (b) Local diagram for $b\sigma_{2n} \in B_{2n+2}$

Figure 28: Fork diagrams associated to $b \in B_{2n} \mapsto b\sigma_{2n} \in B_{2n+2}$

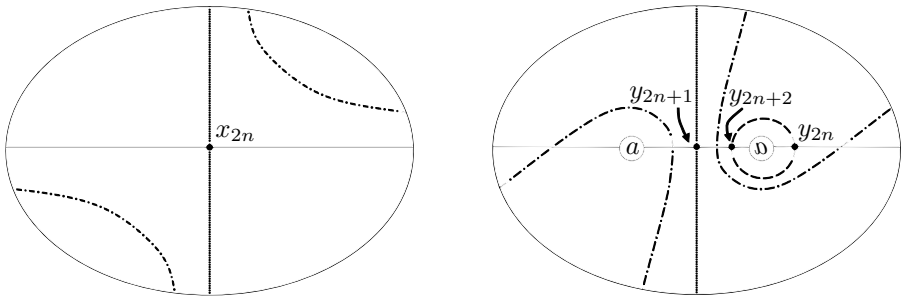

(a) From $b \in B_{2n}$ (b) From $b\sigma_{2n} \in B_{2n+2}$

Figure 29: Heegaard diagrams for $\Sigma(K)\#(S^2 \times S^1)$ covering the fork diagrams in Figure 28

within the local picture. In fact, g_{stab} can be written as a composition $g^b_{stab} \circ g^a_{stab}$ of triangle injections corresponding to the two handleslides. Local regions in domains of 3-gons for these handleslides are exhibited in Figures 31 and 32, respectively. One can verify that they all avoid $\bigtriangledown$.

Remark 36. We don't actually construct a triangle injection associated to the destabilization move. However, by a slight modification to Lemma 28, the chain maps and homotopies on $\widehat{CF}$ induced by destabilization are filtered also.

Notice that the domains for g^b_{stab} are domains of type II 3-gon classes.

$$\begin{aligned} Q(y_{2n+1}y_{2n}\mathbf{v}) &= Q(x_{2n}\mathbf{v}) + 1, & Q(y_{2n+2}\mathbf{z}) &= Q(\mathbf{z}), \\ P(y_{2n+1}y_{2n}\mathbf{v}) &= P(x_{2n}\mathbf{v}), & P(y_{2n+2}\mathbf{z}) &= P(\mathbf{z}), \\ T(y_{2n+1}y_{2n}\mathbf{v}) &= T(x_{2n}\mathbf{v}) + 1, & T(y_{2n+2}\mathbf{z}) &= T(\mathbf{z}). \end{aligned}$$

Stabilization adds two strands, increases ϵ by 1, and decreases w by 1. Thus $s_R(b\sigma_{2n}) = s_R(b)$ and

$$R(y_{2n+1}y_{2n}\mathbf{v}) = R(x_{2n}\mathbf{v}) \quad \text{and} \quad R(y_{2n+2}\mathbf{z}) = R(\mathbf{z}).$$

5.4 Generality of local pictures

It remains to justify that our local pictures above were sufficiently general:

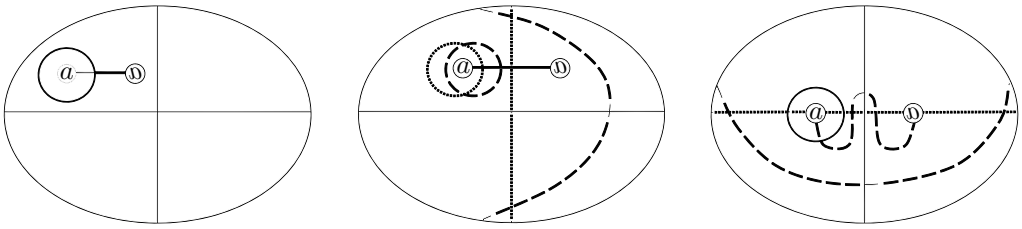

(a) Stabilization (b) $\boldsymbol{\beta}$(dashed) $\mapsto$ $\boldsymbol{\beta}'$(dotted) (c) $\boldsymbol{\alpha}$(dashed) $\mapsto$ $\boldsymbol{\alpha}'$(dotted)

Figure 30: Stabilization and two handleslides connecting Heegaard diagrams for b and $b\sigma_{2n}$

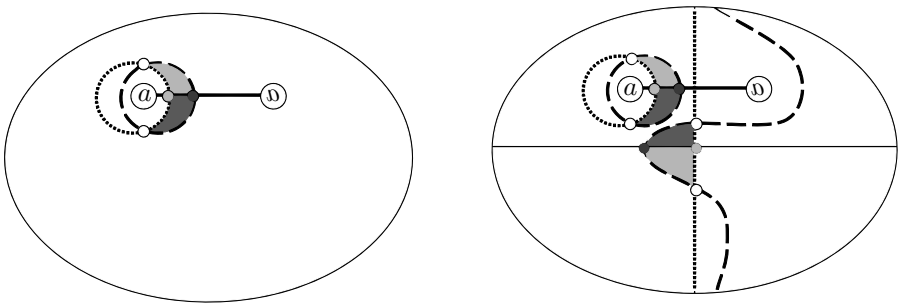

(a) $x_{2n+1} \mapsto w_{2n+1}$ (b) $x_{2n}x_{2n+1} \mapsto w_{2n}w_{2n+1}$

Figure 31: Local regions in domains of type I 3-gons for g^a_{stab}. White dots are components of $\boldsymbol{\theta}_{\boldsymbol{\beta}\boldsymbol{\beta}'}, \boldsymbol{\theta}_{\boldsymbol{\beta}'\boldsymbol{\beta}} \in \mathbb{T}_{\boldsymbol{\beta}} \cap \mathbb{T}_{\boldsymbol{\beta}'}$.

(i) There could be some $u \in \widetilde{\mathcal{Z}}$ such that $u\mathbf{x} \in \mathcal{Z}$ and one of the loops used to compute gradings for $u\mathbf{x}$ contain vertical arcs that pass through the local diagram, as shown in Figure 34. This scenario wasn't accounted for in Section 5.2, but one can verify that the grading contributions of such arcs aren't affected by Birman moves.

(ii) We only included one β arc intersecting the interior of each α arc which is entirely contained in the local area. Multiple β arcs intersecting the interior of the same α arc can be isotoped to be very close to one another and thus behave identically under moves.

(iii) We assumed above that all β arcs shown belong to distinct β_i. If two β arcs share the same β_i, then fewer Bigelow generators are allowed.

(iv) The local pictures in Section 5.2 never have handles passing through them. A handle bh_i contributes a vertical pass-through arc to each loop associated to a point on β_i.

(v) For each Birman move, we chose particular entrance trajectories for β arcs terminating inside the local picture (i.e. from above or from below). For arcs terminating at punctures near the boundary of the local picture, we can modify the entrance trajectory by applying an isotopy to the β arc and shrinking the scope of the picture (see Figure 35).

Entrance trajectories of β arcs terminating far from the boundary can be modified in the same way, but at the expense of adding a pass-through arc to the local picture (see Figure 36).

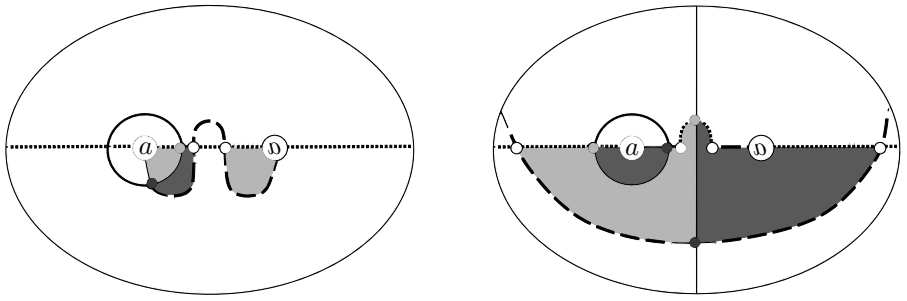

(a) $w_{2n+1} \mapsto y_{2n+2}$ (b) $w_{2n} w_{2n+1} \mapsto y_{2n+1} y_{2n}$

Figure 32: Local regions in domains of the type II 3-gons for g^b_{stab} and $g^b_{stab^{-1}}$. White dots are components of $\boldsymbol{\theta}_{\boldsymbol{\alpha}\boldsymbol{\alpha}'}, \boldsymbol{\theta}_{\boldsymbol{\alpha}'\boldsymbol{\alpha}} \in \mathbb{T}_{\boldsymbol{\alpha}} \cap \mathbb{T}_{\boldsymbol{\alpha}'}$.

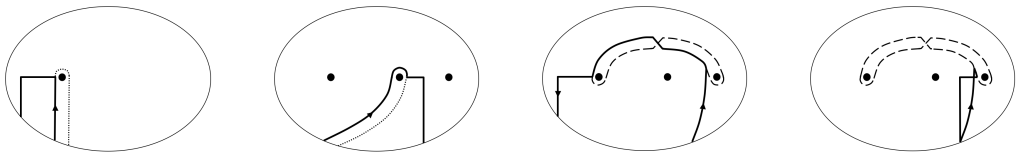

(a) x_{2n} (b) y_{2n+1} (c) y_{2n} (d) y_{2n+2}

Figure 33: Loops for elements of $\mathcal{Z}$ affected by $b \in B_{2n} \leftrightarrow b\sigma_{2n} \in B_{2n+2}$

6 The left-handed trefoil and the lens space $L(3,1)$

The fork diagram for the left-handed trefoil obtained from $\sigma_2^3 \in B_4$ induces the admissible Heegaard diagram $\left(\Sigma_2, \{\widehat{\alpha}_1, \widehat{\alpha}_2\}, \{\widehat{\beta}_1, \widehat{\beta}_2\}, +\infty\right)$ for $L(3,1)\#(S^1 \times S^2)$ shown in Figure 37. Label the intersections on $\widehat{\alpha}_1$ from left to right as $s', t', x_2, t, s,$ and x_1, and label those on $\widehat{\alpha}_2$ from bottom top as $x_4, v', u', x_3, u,$ and v.

Let's perform the calculation with $\mathbb{Z}/2\mathbb{Z}$ coefficients; this can be done combinatorially, since the diagram in Figure 37 is **nice** in the sense of [15].

The differential is thus

$$\widehat{\partial}(x_2x_3) = ut' + u't, \quad \widehat{\partial}(ut) = sx_3 + vx_2, \quad \widehat{\partial}(ut') = \widehat{\partial}(u't) = sv' + s'v,$$
$$\widehat{\partial}(u't') = s'x_3 + v'x_2, \quad \widehat{\partial}(s'v') = \widehat{\partial}(sx_3) = \widehat{\partial}(vx_2) = u'x_1 + t'x_4,$$
$$\widehat{\partial}(s'v) = \widehat{\partial}(sv') = x_1x_4 + x_1x_4 = 0, \quad \widehat{\partial}(v'x_2) = \widehat{\partial}(s'x_3) = \widehat{\partial}(sv) = tx_4 + ux_1,$$
$$\text{and} \quad \widehat{\partial}(u'x_1) = \widehat{\partial}(t'x_4) = \widehat{\partial}(x_1x_4) = \widehat{\partial}(tx_4) = \widehat{\partial}(ux_1) = 0.$$

Now recall that $L(3,1)$, has three Spin^c structures $\mathfrak{s}_i$, $i = 0, 1, 2$. These induce three Spin^c structures on $L(3,1)\#(S^1 \times S^2)$ given by $\mathfrak{s}_i \# \mathfrak{s}$, where $\mathfrak{s}$ is the unique torsion Spin^c-structure on $S^2 \times S^1$. One should observe that the diagram in Figure 37 can be related via handleslides to one which is the disjoint union of a diagram for $\Sigma(K)$ and the usual admissible genus-one diagram for $S^2 \times S^1$. As

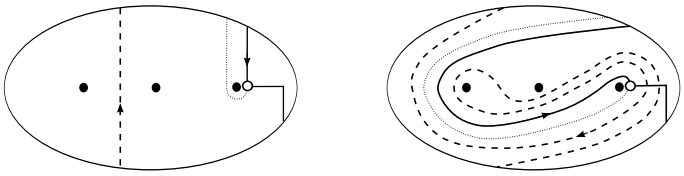

(a) Grading loop for $u\mathbf{x}$ (b) Grading loop for $u'\mathbf{x}$

Figure 34: The effect of the move $b \mapsto bB$ on a pass-through arc appearing in a grading loop

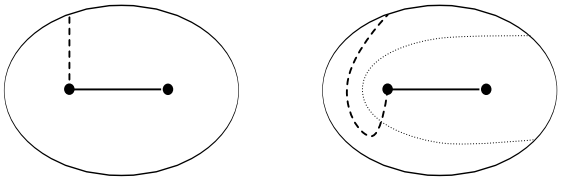

(a) Dashed arc ought to enter from below (b) New local picture has dotted boundary

Figure 35: Modifying the entry trajectory of a β arc terminating near the boundary

a result, all generators $\mathbf{x}$ in Figure 37 have $\mathfrak{s}_{+\infty}(\mathbf{x}) = \mathfrak{s}_{\mathfrak{i}} \# \mathfrak{s}$. They partition this set of generators as

$$\begin{aligned}
\mathfrak{U}_0 &= \{x_2x_3, ut', u't, s'v, sv', x_1x_4\},\\
\mathfrak{U}_1 &= \{ut, s'v', sx_3, vx_2.u'x_1, t'x_4\},\\
\mathfrak{U}_2 &= \{u't', v'x_2, s'x_3, sv, tx_4, ux_1\}.
\end{aligned}$$

Notice that the differential always lowers the R-grading by 1 in this case, and thus the left-handed trefoil is evidently ρ-degenerate. The R-grading then provides an absolute Maslov grading on the group $\widehat{HF}(L(3,1)\#(S^1 \times S^2); \mathbb{Z}/2\mathbb{Z})$.

One can see that a set of generators for $\widehat{HF}(L(3,1)\#(S^1 \times S^2); \mathbb{Z}/2\mathbb{Z})$ is

$$\{s'v, x_1x_4, s'v' + sx_3, u'x_1, sv + s'x_3, ux_1\},$$

and thus the homology group decomposes with respect to the R-grading as

$$\widehat{HF}(L(3,1)\#(S^1 \times S^2); \mathbb{Z}/2\mathbb{Z}) = \left[(\mathbb{Z}/2\mathbb{Z})^{\oplus 3}\right]_{R=3/2} \oplus \left[(\mathbb{Z}/2\mathbb{Z})^{\oplus 3}\right]_{R=1/2}.$$

7 Future directions

7.1 Relationship with $Kh_{symp,inv}$

Given a pointed Heegaard diagram $\mathcal{H}$ for $\Sigma(K)\#(S^2 \times S^1)$ coming from a braid, we saw that the filtration ρ can only be defined on generators in torsion Spin^c structures. It would be interesting to investigate whether Heegaard diagrams encountered in this context actually contain generators in non-torsion Spin^c structures. It is possible that E_1 is in fact all of $Kh_{symp,inv}(K)$; in particular, we would obtain that when K is ρ-degenerate,

$$\widehat{HF}(\Sigma(K)\#(S^2 \times S^1)) \cong Kh_{symp,inv}(K).$$

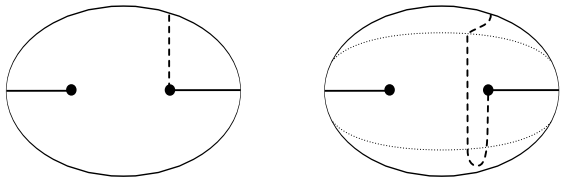

(a) Dashed arc ought to enter from below

(b) New local picture has dotted boundary

Figure 36: Modifying the entry trajectory of a β arc terminating far from the boundary

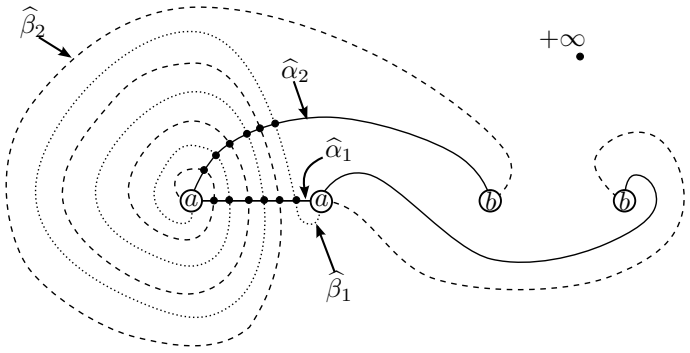

Figure 37: The Heegaard diagram for $L(3,1)\#(S^1 \times S^2)$ obtained from $\sigma_2^3 \in B_4$

7.2 The Khovanov-Heegard Floer spectral sequence

Ozsváth and Szabó showed in [11] that the groups $\widehat{HF}(\Sigma(L))$, $\widehat{HF}(\Sigma(L_0))$, and $\widehat{HF}(\Sigma(L_1))$ fit into a long exact sequence:

$$\ldots \longrightarrow \widehat{HF}(\Sigma(L_0) \longrightarrow \widehat{HF}(\Sigma(L_1) \longrightarrow \widehat{HF}(\Sigma(L) \longrightarrow \ldots$$

where the diagrams for L_0 and L_1 exhibit the two smooth resolutions of some crossing c in L and coincide with L away from c. The existence of this sequence is a consequence of the surgery exact sequence for $\widehat{HF}$, and Ozsváth and Szabó use it to construct a spectral sequence whose E^2 term is isomorphic to the reduced Khovanov homology $\widetilde{Kh}(\overline{L};\mathbb{Z}/2\mathbb{Z})$ of the mirror of L and which converges to the Heegaard Floer homology group $\widehat{HF}(\Sigma(L);\mathbb{Z}/2\mathbb{Z})$. Let $\delta = (j-i)$ denote the quantum grading, the collapse of the bigrading on the group

$$\widetilde{Kh}(L) = \bigoplus_{i,j} \widetilde{Kh}^{i,j}(L).$$

It was shown in [8] that the class of quasi-alternating links is Khovanov-thin, with $\widetilde{Kh}^{i,j}(L) \neq 0$ only if $\delta = (j-i) = -\sigma(L)/2 = \sigma(\overline{L})/2$. Notice that when L is a two-bridge link, this is exactly the $\underline{R}$-level supporting $\widehat{HF}(\Sigma(\overline{L}))$.

Baldwin [1] conjectured the existence of an induced δ-grading on higher pages in the spectral sequence, and Greene [4] conjectured that a term arising in his spanning tree model could provide a quantum grading on $\widehat{HF}(\Sigma(K))$. If the gradings conjectured by Greene and Baldwin indeed exist, it would be interesting to compare them to the R-grading for ρ-degenerate knots.

Acknowledgments

It is my pleasure to thank Ciprian Manolescu for suggesting this problem to me and for his invaluable guidance as an advisor. I would also like to thank Liam Watson and Tye Lidman for some instructive discussions, Stephen Bigelow for some helpful email correspondence related to his paper [2], Yi Ni for some useful comments regarding relative Maslov gradings.

This paper has been rewritten from a previous version to account for an update to [18]. I am indebted to Ivan Smith for pointing out this change.

References

[1] J. Baldwin, *On the spectral sequence from Khovanov homology to Heegaard Floer homology*, Electronic pre-print, arXiv:0809.3293v4 (2009).

[2] S. Bigelow, *A homological definition of the Jones polynomial*, Geom. topol. monogr. vol. 4, 2002, pp. 29–42.

[3] J. Birman, *On the stable equivalence of plat representations of knots and links*, Canad. J. Math. **28** (1976), 264–290.

[4] J. Greene, *A spanning tree model for the Heegaard Floer homology of a branched double-cover*, Electronic pre-print, arXiv:math/0805.1381v1 (2008).

[5] M. Kontsevich, *Homological algebra of mirror symmetry*, Proceedings of the International Congress of Mathematicians (Zürich, 1994), 1978, pp. 120–139.

[6] R. Lipshitz, *A cylindrical reformulation of Heegaard Floer homlogy*, Geom. Topol. **10** (2006), 955–1097.

[7] C. Manolescu, *Nilpotent slices, Hilbert schemes, and the Jones polynomial*, Duke Math. J. **132** (2006), 311–369.

[8] C. Manolescu and P. Ozsváth, *On the Khovanov and knot Floer homologies of quasi-alternating links*, Proceedings of the 14th gökova geometry-topology conference, 2007, pp. 60–81.

[9] P. Ozsváth and Z. Szabó, *Holomorphic disks and three-manifold invariants: Properties and applications*, Annals of Math. **159** (2004), 1159–1245.

[10] ———, *Holomorphic disks and topological invariants for closed three-manifolds*, Annals of Math. **159** (2004), 1027–1158.

[11] ———, *On the Heegaard Floer homology of branched double-covers*, Advances in Math. **194** (2005), 1–33.

[12] ———, *Holomorphic triangles and invariants for smooth four-manifolds*, Advances in Math. **202** (2006), 326–400.

[13] J. Robbin and D. Salamon, *The Maslov index for paths*, Topology **4** (1993), 827–844.

[14] S. Sarkar, *Maslov index formulas for Whitney n-gons*, Electronic pre-print, arXiv:math/0609673v3 (2010).

[15] S. Sarkar and J. Wang, *An algorithm for computing some Heegaard Floer homologies*, Annals of Math. **171** (2010), 1213–1236.

[16] P. Seidel, *Graded Lagrangian submanifolds*, Bull. Soc. Math. France **128** (2000), 103–146.

[17] P. Seidel and I. Smith, *A link invariant from the symplectic geometry of nilpotent slices*, Duke Math. J. **134** (2006), 453–514.

[18] ———, *Localization for involutions in Floer cohomology*, Electronic pre-print, arXiv:1002.2648 (2010).

[19] J. Waldron, *An invariant of link cobordisms from symplectic Khovanov homology*, Electronic pre-print, arXiv:0912.5067 (2009).